WHITE PAPER

FEBRUARY 2022

COMING BACK TO REALITY: A PROPOSAL FOR REAL-WORLD ACCURACY REQUIREMENTS FOR VEHICLE ON-BOARD FUEL AND ENERGY CONSUMPTION MONITORING

Jan Dornoff, Nikiforos Zacharof

www.theicct.org

communications@theicct.org

twitter @theicct

THE INTERNATIONAL COUNCIL ON CLEAN TRANSPORTATION

BEIJING | BERLIN | SAN FRANCISCO | SÃO PAULO | WASHINGTON

ACKNOWLEDGMENTS

The authors thank the employees of the Technical University of Vienna in Austria for their effective collaboration in conducting vehicle tests. The authors also thank HORIBA Automotive for generously lending the ultrasonic fuel flow meters free of charge. The authors express their gratitude to all internal and external reviewers of this report for their guidance and constructive comments, with special thanks to Anna Krajinska (Transport & Environment), Georgios Fontaras (Joint Research Centre of the European Commission), Leo Breton (HORIBA Automotive), Iddo Riemersma (Sidekick Project Support), and John German, Peter Mock, Pierre-Louis Ragon, Felipe Rodriguez, and Zifei Yang (International Council on Clean Transportation). Their reviews do not imply endorsement, and any errors are the authors' own.

Editor: Amy Smorodin

For additional information:
International Council on Clean Transportation Europe
Fasanenstrasse 85, 10623 Berlin, Germany

Funding for this work was generously provided by the European Climate Foundation.

communications@theicct.org | www.theicct.org | @TheICCT

EXECUTIVE SUMMARY

To prevent continued widening of the gap between official fuel consumption values and those observed during real-world driving, the European Commission is required to monitor and develop mechanisms to counteract the trend. To do so, the European Commission plans to use real-world data from on-board fuel and energy consumption monitoring (OBFCM) devices, which are mandatory for most light-duty vehicles since January 2021.

For obtaining reliable real-world data, it is necessary that OBFCM data be accurate. Accuracy requirements are currently defined only for fuel volume consumed, not distance-specific fuel consumption, and only when measured during type-approval testing in the laboratory. It is therefore necessary to develop OBFCM accuracy requirements for real-world driving for fuel volume and distance driven to be able to calculate real-world fuel consumption.

Data accuracy that can reasonably be required for verification testing is affected by three main factors: the accuracy of the OBFCM device itself when tested at reference conditions, uncertainty of the method used to verify OBFCM accuracy, and uncertainties introduced by differences between verification test conditions and reference conditions. This study provides evidence on the level of uncertainty of these elements and develops recommendations for future OBFCM data accuracy requirements.

To generate independent data for this analysis, we performed an extensive vehicle test program on three modern passenger cars equipped with OBFCM devices. The vehicles were tested on chassis dynamometer and on public roads. During all tests, the OBFCM values were recorded together with fuel consumption and driven distance measured independently by different verification methods. For estimating the effect of using market fuel instead of reference fuel and variability of wheel dimensions on the OBFCM data accuracy, a theoretical analysis was conducted.

Based on our analysis, we recommend the combined OBFCM fuel consumption and distance accuracy requirements presented in Figure ES 1. Depending on whether the OBFCM accuracy verification tests are performed on chassis dynamometer or on public roads, and whether the tests are performed under reference conditions, different uncertainties are considered.

Test environment	OBFCM parameter	OBFCM* accuracy requirements: Currently defined for type approval	OBFCM* accuracy requirements: Recommended when using… Reference wheels / Reference fuel	OBFCM* accuracy requirements: Recommended when using… Random wheels / Market fuel
Chassis dynamometer testing	Fuel consumption	±5.0%	±1.6%	Diesel: ±1.7% Gasoline: ±2.7%
Chassis dynamometer testing	Distance	None	±0.6%	±1.9%
Real-world testing	Fuel consumption	None	±3.3%	Diesel: ±3.3% Gasoline: ±3.9%
Real-world testing	Distance	None	±0.7%	±1.1%

*On-board fuel- and energy-consumption monitoring

Figure ES 1. Recommendations for OBFCM fuel consumption and distance accuracy when verified on chassis dynamometer and in real-world driving. Different accuracy recommendations apply when reference fuel and wheels or market fuel and random wheels are used.

For plug-in hybrid electric vehicles (PHEVs), the OBFCM records electric energy consumption as well as fuel consumption and distance in PHEV-specific operating modes. Our analysis revealed that under the current regulatory provisions, the possibility for assessing the accuracy of these parameters is limited. Nevertheless, our analysis leads to the following recommendations for improving OBFCM regulation for PHEVs:

» Accuracy requirements for the PHEV-specific OBFCM parameters should be defined. Our results suggest that the same requirements as presented in Figure ES 1 should be used for the PHEV operating mode-specific fuel consumption and distance parameters.

» We also recommend defining accuracy requirements for recharged grid energy. However, for accuracy verification, it is necessary that the OBFCM recharged grid energy value be reported by the vehicle with a higher resolution than currently defined.

» For verifying OBFCM accuracy in PHEV operating modes, the vehicle needs to continuously communicate the current operating mode and battery energy flow at the OBD interface. Furthermore, a safe and standardized access for measuring the voltage and current of the high-voltage battery is needed.

Based on the experience and insights gained during the project, we also offer the following recommendations to amend the regulation for making OBFCM data more robust and reliable:

» Accumulated second-by-second OBFCM values should equal the OBFCM lifetime values.

» OBFCM values should not have a systematic offset.

» It should be clarified in the regulation that the volumetric OBFCM fuel consumption relates to a fuel temperature of 15°C.

TABLE OF CONTENTS

ABBREVIATIONS

A/C	air conditioning
AFM	air flow meter
BSG	belt starter generator
CADC150	Common Artemis 150 Drive Cycle
CD	charge depleting
CI	charge increasing
CO_2	carbon dioxide
CoC	certificate of conformity
CVS	constant volume sampling
DGPS	differential global positioning system
EFM	exhaust flow meter
FFM	fuel flow meter
GPS	global positioning system
HVBM	high voltage breakout module
ICE	internal combustion engine
LHV	lower heating value
LoA_{95}	95% level of agreement
NO_xS	NO_x sensor
NYCC	New York City Cycle
O_2	oxygen
O_2+AFM	carbon balance method based on oxygen concentration and air flow meter
OBD	on-board diagnostic
OBFCM	on-board fuel and energy consumption monitoring
PEMS	portable emissions measurement system
PHEV	plug-in hybrid electric vehicle
RDE	real driving emissions
SoC	state of charge
SUV	sport utility vehicle
THC	total hydrocarbons
TPMS	tire pressure monitoring system
US06	US06 drive cycle
VM	verification method
WLTC	Worldwide harmonized Light vehicles Test Cycle
WLTP	Worldwide harmonized Light vehicles Test Procedure

1. INTRODUCTION

With the goal of reducing carbon dioxide (CO_2) emissions from transport, the European Union (EU) introduced binding type-approval CO_2 targets for passenger cars in 2009 and for light commercial vehicles in 2011. Due to continued strengthening of these targets, the type-approval CO_2 emissions, determined by laboratory testing, have been reduced over time. At the same time, the gap between the type-approval values and the CO_2 emissions reported for real-world vehicle usage increased from 8% in 2001 and to almost 40% in 2017 (Tietge et al., 2019). This gap undermines the effectiveness of the CO_2 standards in reducing road transport-related greenhouse gases.

To ensure that future reductions in type-approval CO_2 values have the desired effect on real-world emissions, the latest CO_2 target regulation (EU) 2019/63[1] requires the European Commission (EC) to collect real-world fuel consumption data as a proxy for CO_2 emissions (Regulation (EU) 2019/631, 2019). The data will be used to monitor real-world CO_2 emissions to inform polices intended to counteract the widening of the gap.

As a prerequisite, the EC amended the type-approval regulation (EU) 2017/1151 with a provision that requires manufacturers to install on-board fuel and energy consumption monitoring (OBFCM) devices in all new light duty vehicles.[2] The OBFCM devices permanently determine and record the data shown in Table 1 on board each vehicle. Based on the total fuel consumption and mileage over a vehicle's lifetime, the average distance-specific real-world fuel consumption can then be calculated and compared with the type-approval values. For plug-in hybrid electric vehicles (PHEVs), additional parameters specific to PHEV operating modes are required to be recorded.

To yield reliable real-world data, it is necessary that the OBFCM data be accurate. For this purpose, the regulation contains a verifiable accuracy requirement of ±5% for volumetric fuel consumption. However, since fuel consumption is determined only during type approval on the chassis dynamometer, the requirement sets accuracy limits only for this test. Since the expressed goal for using OBFCM data is determining the real-world fuel consumption, it is necessary to define verifiable accuracy requirements for real-world driving as well. Furthermore, the accuracy of the distance driven needs to be ensured to precisely calculate the distance-specific fuel consumption in liters per 100 kilometers. To address this topic, the EC established a task force in 2020 for developing OBFCM real-world accuracy requirements for type-approval and in-service conformity testing.

Table 1. Lifetime on-board fuel and energy consumption monitoring (OBFCM) data to be determined and stored in a vehicle.

OBFCM parameter to be accumulated over lifetime	Unit	Applicable to
Fuel consumption	liters	All vehicles
Total mileage	km	All vehicles
Fuel consumption in battery-depleting operation	liters	Only PHEVs
Fuel consumption in user selectable battery-charging operation	liters	Only PHEVs
Mileage in battery-depleting operation with combustion engine on	km	Only PHEVs
Mileage in battery-depleting operation with combustion engine off	km	Only PHEVs
Mileage in user selectable battery-charging operation	km	Only PHEVs
Total electric grid energy supplied to the battery	kWh	Only PHEVs

1 Regulation (EC) 2019/631 sets the CO_2 performance targets for passenger cars and light commercial vehicles for the years 2025 and 2030. It was adopted in 2019 and repeals the former regulations (EC) 443/2009 and (EU) 510/2011.

2 Applying an OBFCM device is required for all new type approved M1 and N1 class I vehicles starting January 2020 and one year later for all new vehicles of these categories. For N1 class II and III, the introduction of OBFCM devices is delayed by one year.

This paper is intended to provide independent input to this task force. To generate data for our analysis, we performed extensive vehicle testing on three modern passenger cars, all type-approved to the latest Euro 6d stage, which requires the vehicles to have OBFCM devices. The test vehicles were equipped with instruments for measuring the fuel and electric energy as well as the distance driven and a data logger to record the OBFCM data. The test program included laboratory tests covering a wide range of driving styles and ambient temperatures as well as real-world tests performed on public roads.

As shown in Figure 1, we first analyzed the accuracy of the methods intended for verifying OBFCM accuracy during on-road driving. We then assessed the accuracy of the test vehicles' OBFCM devices both on chassis dynamometer and during real-world driving. Effects on OBFCM accuracy that were not investigated by testing were assessed theoretically. Based on market fuel data, we investigated how using market fuel instead of reference fuel can affect OBFCM accuracy. We also assessed how wheel dimensions, tire wear, and pressure can affect OBFCM distance accuracy. Based on the results, we developed recommendations for future OBFCM accuracy requirements.

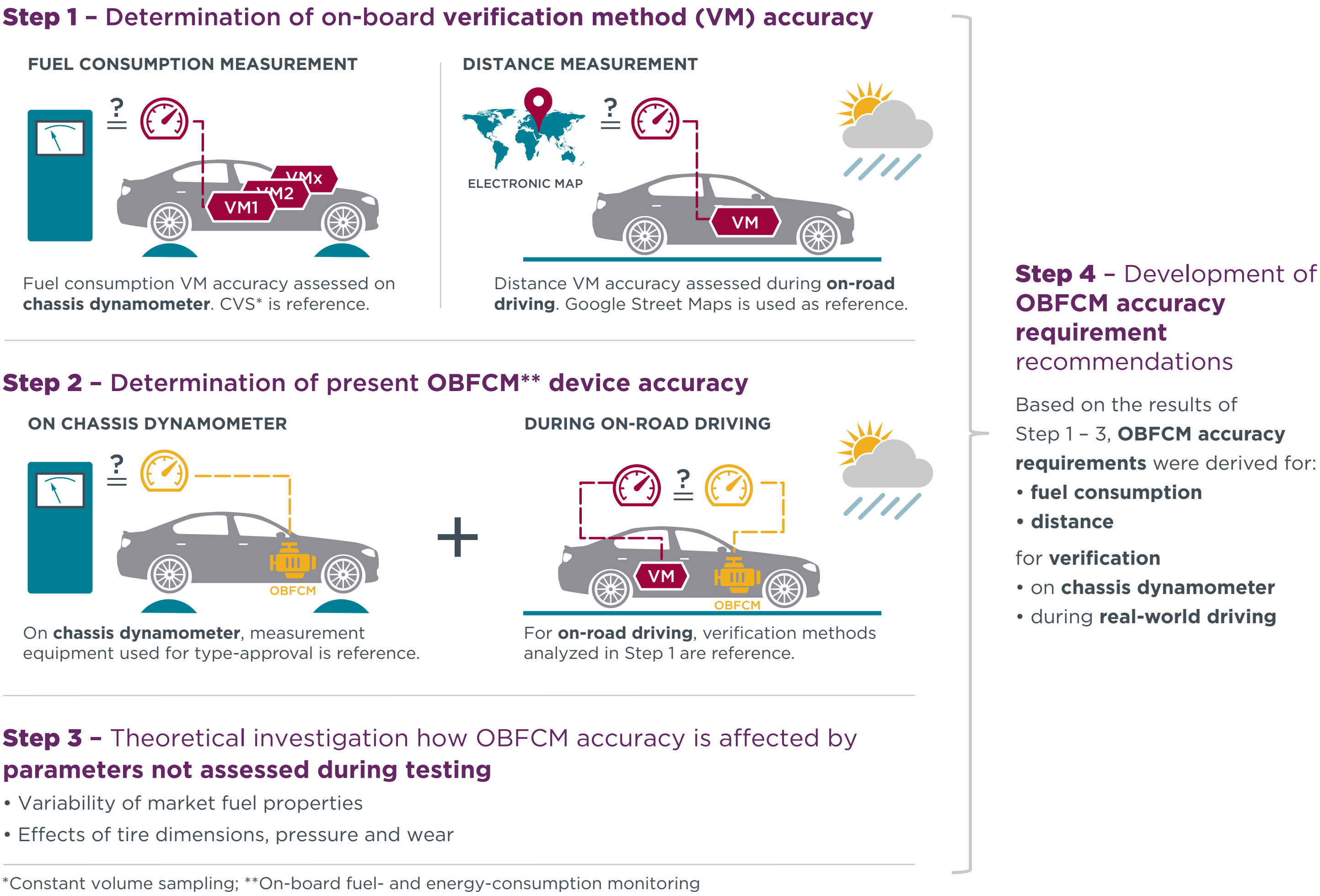

Figure 1. Process applied for developing recommendations for future OBFCM accuracy requirements.

The paper is structured as follows:

» Section 2 provides an overview of the methodology applied, including a description of the test vehicles, the verification methods investigated, and the tests performed.

» Section 3 presents the results of our data analysis and the derived conclusions.

» The results are summarized in section 4, and we offer recommendations as input to the EC task force and for improving the current OBFCM regulation.

2. METHODOLOGY

This section explains the approach taken to achieve the project goals presented in section 1. First, we describe the different methods used for determining fuel and energy consumption as well as distance driven on chassis dynamometer and during real-world driving, the basis for verifying OBFCM accuracy. We then provide information on the three test vehicles and how they were equipped with measurement devices. After an overview of the chassis dynamometer and real-world tests performed, we discuss how test data was processed and analyzed to derive our recommendations for future OBFCM accuracy requirements.

2.1. METHODS USED FOR DETERMINING FUEL CONSUMPTION AND DISTANCE DRIVEN DURING LABORATORY AND ON-ROAD TESTING

A comparison of real-world fuel consumption with type-approval values requires measurement of both volumetric fuel consumption and distance driven. For this purpose, the reference distance for verifying OBFCM distance during real-world driving was calculated based on global positioning system (GPS) coordinates measured by a differential GPS (DGPS) device, further described in section 2.4.2. On chassis dynamometer, the distance determined by the laboratory equipment during type approval was used as reference.

For verifying OBFCM fuel consumption accuracy during real-world driving, four OBFCM-independent measurement methods were investigated in this project, two of them based on exhaust oxygen concentration and air flow measurement. During the chassis dynamometer tests, fuel consumption was also measured using constant volume sampling (CVS), the method applied during type approval. The methods investigated in this project are described in more detail in the following sections.

2.1.1. Constant volume sampling bag analysis (CVS)

During type approval, fuel consumption and pollutant emissions are determined on the chassis dynamometer using the constant volume sampling bag analysis method shown in Figure 2. The CVS method directly provides the mass of each measured exhaust component emitted during the test. Using the driven distance measured by the chassis dynamometer, distance-specific emissions are calculated.

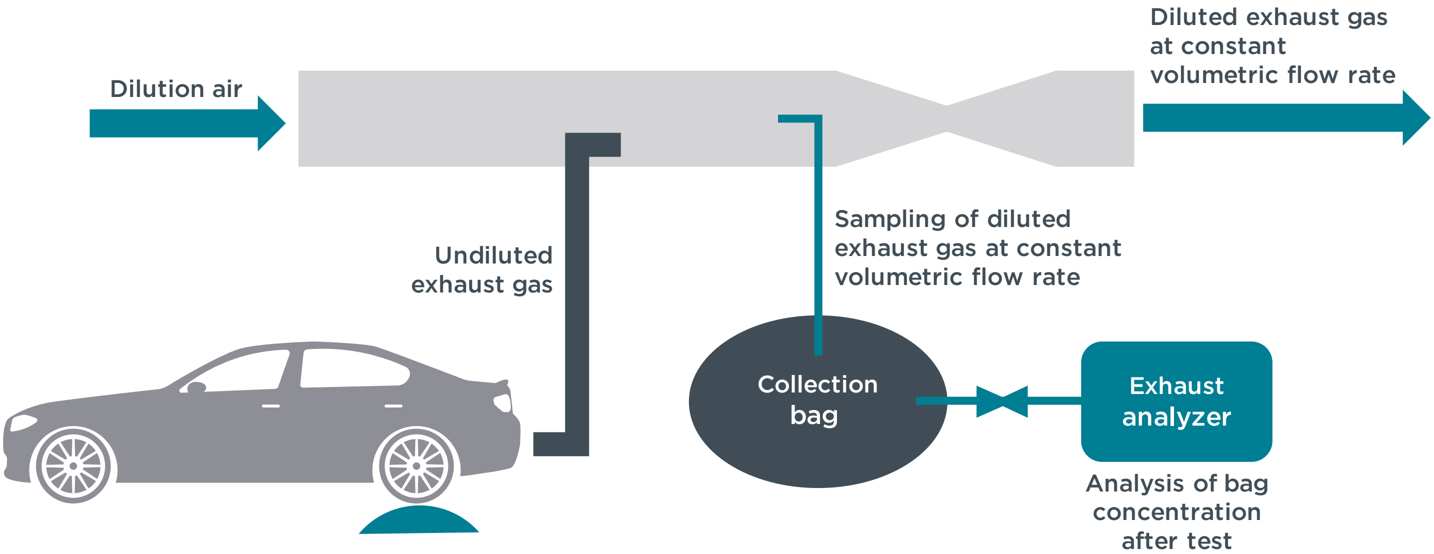

Figure 2. Schematic of constant volume sampling (CVS) for pollutant emission mass determination on chassis dynamometer

Based on this information, the mass of fuel burned over the test cycle is calculated by balancing the carbon content of the fuel with the carbon content derived from the carbon-containing exhaust species: CO_2, carbon monoxide (CO) and total hydrocarbons (THC). This requires knowledge of the fuel composition. For calculating volumetric fuel consumption from mass, fuel density at a reference temperature defined by the type-approval regulation at 15°C is used.

The advantage of this method is the physical integration of the emissions in the bag, providing the test average pollutant concentrations, eliminating the need for any time alignment of pollutant concentrations with exhaust mass flow rates.

2.1.2. Portable emissions measurement system (PEMS)

The CVS method is usually suited only for stationary applications. During real-world driving, portable emission measurement systems (PEMS) can be used to measure individual emission species concentrations in undiluted exhaust gas at the vehicle tailpipe. To calculate emission mass flows, the exhaust mass flow is needed, measured by an exhaust flow meter (EFM). For calculating precise emission mass flow rates, a good time alignment between exhaust mass flow and pollutant concentration signal is essential, introducing an element of measurement uncertainty. The direct results of a PEMS measurement are the exhaust species mass flow rates.

For accurately deriving fuel mass flow through a carbon balance, the carbon content in the exhaust as well as the fuel composition is needed. While PEMS can measure hydrocarbons with additional analyzers, the light duty real-driving emissions (RDE) regulation requires the measurement only of nitrogen oxides (NO_x), $CO_{2,}$ and CO. However, since the THC concentration is usually many orders of magnitude smaller than the CO_2 concentration, the error in fuel mass introduced by assuming a 0 ppm THC concentration is very small and considered negligible for this study.

As with the CVS method, knowledge of the fuel density at the reference temperature of 15°C is required to calculate the volumetric fuel consumption.

2.1.3. Ultrasonic fuel flow rate meter

In this project we had the opportunity to test two identical Sentronics fuel flow meters (FFMs), branded FlowSonic ULF, supplied by HORIBA Automotive in conjunction with a technical partnership. The tested FFMs are prototype versions of a series product adapted for flow rates encountered in light-duty vehicles. The sensors use the principal of ultrasonic flow measurement, which relies on determining the travel time of an ultrasound wave through the fluid over a defined length along the flow direction. The travel time linearly depends on the flow velocity. By measuring the travel time both with and against the flow direction, the effects of temperature and viscosity can be eliminated, and the sensor directly provides the flow velocity. In combination with a known cross section of the flow tube, the volumetric flow rate can then be calculated (Bonfig et al., 2014).

For comparison with official fuel consumption figures, the measured volumetric fuel flow needs to be normalized to the type-approval reference temperature of 15°C. For this purpose, the fluid temperature is continuously measured by the flow meter, and a fuel type-specific linear temperature-density dependency is applied (Wolf, 2015).

The current version of the sensor is designed only for one-way fuel supply systems, the standard for most gasoline engines. For systems with both a supply and a return line, as encountered in most diesel vehicles, the senor is not suitable in its current version.

2.1.4. Carbon balance using a wideband oxygen sensor and air or exhaust mass flow meter

The instantaneous fuel mass flow rate can also be determined indirectly based on the exhaust oxygen concentration and the engine's air or exhaust mass flow rate, provided the fuels' hydrogen-to-carbon and oxygen-to-carbon ratios are known.

When available, we performed the calculation based on signals at the OBD interface. While this method comes with the lowest installation effort and cost, it has several drawbacks. First, it relies on information provided by the vehicle and can therefore not be considered independent. Second, data at the OBD interface is not broadcast continuously but must be polled, which leads to limited data transfer rates and is prone to time misalignment. Third, the resolution of some OBD signals is low, leading to rounding errors. Last, the signals required for the calculation are not available on all vehicles.

As an alternative to relying on OBD signals, we installed an exhaust oxygen sensor, which can measure the equivalent oxygen concentration in both lean and rich exhaust gas. For an independent air flow measurement, we recorded the raw signal from the vehicle's air flow meter (AFM), as explained in section 2.2.2.

2.2. TEST VEHICLE SELECTION AND INSTRUMENTS INSTALLED

For this analysis, we tested three modern passenger vehicles, all of them type approved according to the latest Euro 6d ISC-FCM emissions standard. This ensured that all vehicles were equipped with OBFCM devices. The vehicles were also selected to cover a range of today's most popular powertrain layouts. We selected a BMW X1 xDrive25e gasoline plug-in hybrid electric vehicle (PHEV), a diesel engine-powered Mercedes C220d T, and a 48V mild-hybrid gasoline Audi A3 30 TFSI. Table 2 displays the most relevant technical parameters of the test vehicles.

Table 2. Test vehicle parameters

Parameter	BMW X1 xDrive25e	Mercedes C220d T	Audi A3 30 TFSI
Powertrain architecture	Plug-in hybrid	Internal combustion engine only	48V mild hybrid
Fuel type[a]	Gasoline (E10)	Diesel (B7)	Gasoline (E10)
Transmission	DCT[b] - 6 gears	Automatic - 9 gears	DCT[b] - 7 gears
Powered axle(s)	Electric all-wheel drive[c]	Rear-wheel drive	Front-wheel drive
Chassis type	Sport utility vehicle (SUV)	Station wagon	Hatchback
Actual mass (WLTP)[d]	1,871 kg	1,715 kg	1,401 kg
Emission standard (EU) 2018/1832	Euro 6d-ISC-FCM (Euro 6 AP)	Euro 6d-ISC-FCM (Euro 6 AP)	Euro 6d-ISC-FCM (Euro 6 AP)
Fuel consumption –combined (WLTP)	1.8 l/100km[e]	5.6 l/100km	5.4 l/100km
CO_2 emissions - combined (WLTP)	41 g/km[e]	147 g/km	122 g/km
Engine capacity	1,499 cm^3	1,950 cm^3	999 cm^3
Cylinder configuration and number	In-line 3	In-line 4	In-line 3
Fuel tank capacity	36 liters	41 liters	45 liters
Rated power – Internal combustion engine	92 kW	143 kW	81 kW
Rated torque – Internal combustion engine	165 Nm	400 Nm	200 Nm
Rated power – Electric	BSG[f] 15 kW Rear axle[c] 70 kW	N/A	BSG[f] 9.4 kW
Date of first registration	March 2020	July 2020	January 2021
Mileage at test start	~1,000 km	~15,000 km	~200 km

[a] Parameter in parentheses is the fuel type used for type approval.
[b] DCT: Automated double clutch transmission.
[c] The combustion engine powers the front axle; a second electric motor powers the rear axle.
[d] Includes mass of optional equipment, driver, and fuel tank 90% full.
[e] Weighted-combined.
[f] Belt starter generator: The combustion engine alternator can be used both as a generator and an electric motor.

Prior to testing, we equipped the vehicles with the following measurement instruments and data acquisition systems.

2.2.1. Installation of the fuel flow meter

In both gasoline vehicles, the BMW and the Audi, the fuel flow meter was directly installed in the fuel supply line from the tank to the engine. The original fuel piping had two coupling points using standardized quick couplings. One connection was located underfloor where the fuel tank connects to the rigid chassis pipes, and the second was in the engine compartment, where the pipes are flexibly connected by hoses to the engine. Using these coupling points, a fast installation of the sensor was possible. Due to its compact size of 16x7x3.7 cm, it was easy to integrate in the engine compartment of the BMW and underfloor for the Audi.

The FFM could not be used in the Mercedes due to the fuel system layout having both a supply and return line connecting engine and fuel tank.

2.2.2. Oxygen sensor installation and approach taken for air flow rate measurement

For this project, we installed in each vehicle a Continental UniNOx NO_x sensor, which offers simultaneous NO_x and wideband O_2 concentration measurement. The sensors were positioned downstream from the oxidation catalysts.

Considering the high installation effort and cost, we did not use an independent air flow meter for our investigations. Instead, to achieve an independent mass flow measurement and a higher signal resolution than available at the OBD interface, we tapped the vehicle air flow meter signal wires of the BMW and Mercedes and intercepted the raw signals. Under the assumption that the AFM measures accurately on chassis dynamometer during type-approval testing, we derived a transfer curve for converting the raw signal to a flow signal by aligning the intercepted signal with the OBD air flow signal.[3]

The Audi A3 gasoline engine was not equipped with an AFM. Therefore, only a modeled exhaust mass flow signal was available at the OBD interface. To assess the accuracy of the NO_x sensor-based method independent of the uncertainties of a calculated mass flow value, we installed the air box of a 1.5 l Volkswagen gasoline engine, which is identical to the 1.0 l Audi engine component except it includes an AFM. Since the approximate transfer curve of this AFM was known from a former test project (Dornoff & Rodríguez, 2019), a direct measurement of the air mass flow rate of the Audi engine was possible.

It should be noted that on all vehicles the derived AFM transfer curves show a nonlinear behavior and can therefore only approximate the true calibration. This might introduce an error in the air mass flow measurement, especially at the upper and lower flow range boundaries. Furthermore, AFM accuracy is affected by oscillations in the intake air system, which are compensated for only by algorithms in the engine control unit. The air flow signal available to the engine control unit, and thereby to the OBFCM, is therefore expected to have a much higher accuracy than we were able to acquire by tapping the raw sensor signal.

2.2.3. Electric power measurement

For plug-in hybrid vehicles, the OBFCM records the fuel consumption and distance in the various plug-in hybrid operating modes as well as the total electric energy recharged to the battery. For measuring the electric energy consumed and recharged both on chassis dynamometer and during real-world driving, a high-voltage breakout

3 The AFM transfer curve describes the correlation between the air mass flow (physical value) and the sensor output signal.

module (HVBM) of type HV-BM 1.2 was installed in the cables to the traction battery. This module is integrated in the high voltage loop and measures current and voltage simultaneously at frequencies up to 1 MHz and calculates instantaneous power.

2.2.4. Data acquisition

In addition, instantaneous and lifetime OBFCM and other OBD data as well as vehicle and ambient parameters were recorded by an autonomous data logger. The data logger also recorded the GPS coordinates for each real-world test via an integrated DGPS device. Table 3 provides for each of the three tested vehicles an overview of the measurement systems installed and the OBD/OBFCM signals available for calculating fuel flow, traveled distance, and electric energy consumption.

Table 3. Overview of available OBD signals and measurement systems used for fuel flow, distance, and energy consumption determination in the three test vehicles. The determined values are used for verifying the accuracy of the OBFCM lifetime values.

Measurement system/signal	Required for calculation of...	Audi A3 (gasoline)	BMW X1 (gasoline)	Mercedes C-class (diesel)
NO_x sensor + air flow meter	Fuel flow	✓	✓	✓
OBD exhaust air/fuel ratio	Fuel flow	✓	✓	×
OBD air mass flow rate	Fuel flow	×	✓	✓
OBD exhaust mass flow rate	Fuel flow	✓	✓	×
Ultrasonic fuel flow meter	Fuel flow	✓	✓	×
PEMS exhaust flow meter[a]	Fuel flow	✓	✓	✓
PEMS emission analyzer[a]	Fuel flow	✓	✓	✓
Data logger DGPS[b]	Distance	✓	✓	✓
OBD vehicle speed	Distance	✓	✓	✓
High voltage power measurement	Energy consumption	N/A	✓	N/A

[a] Only for real-driving emissions tests and selected chassis dyno tests.
[b] For all real-world tests.

2.3. OVERVIEW OF TESTS PERFORMED

After installing the measurement equipment, the vehicles were transferred to the Institute for Powertrains and Automotive Technology of the Technical University of Vienna, Austria, where the vehicle tests were conducted.

The laboratory tests were performed on a four-wheel chassis dynamometer certified for EU type approval. To assess the accuracy of the OBFCM and the verification methods, various drive cycles with different speed profiles were performed, as shown in Table 4. The test cycles were chosen to represent a wide range of driving patterns, including those considered challenging for on-board fuel consumption determination.

Table 4. Characteristics of chassis dynamometer test types

Cycle Type	Distance [km]	Duration [s]	Average / Max speed [km/h]	$(v \times a)_{pos,\ 95pct}$* $[m^2/s^3]$	Stops per km [-]
WLTC	23.3	1,801	46.5 / 131	12.3	0.30
3xNYCC	5.7	1,794	11.4 / 44	10.2	5.26
CADC150	51.7	3,143	59.2 / 150	16.9	0.37
3xUS06	38.7	1,803	77.2 / 129	27.3	0.39

*95th percentile of the product of instantaneous vehicle speed and acceleration. This parameter is a metric for the dynamicity of a test.

The Worldwide harmonized Light Vehicles Test Cycle (WLTC), used for type approval in the European Union, was performed at -5°C, 23°C and 35°C. For the US06 cycle, chosen to investigate very dynamic driving, three consecutive tests were performed to compensate for the short distance of a single cycle, referred to as 3xUS06. The 3xNYCC test, consisting of three consecutive New York City Cycles (NYCCs), was chosen to investigate the accuracy when operating at low engine load and frequent stop-start events. However, since the 3xNYCC is not representative for real-driving emission tests, which we expect will be used for real-world OBFCM accuracy verification, we present the 3xNYCC test results but exclude them when deriving accuracy requirement recommendations. The Common Artemis Drive Cycle 150 (CADC150) with a maximum speed of 150 km/h was selected to include a mixed driving cycle with higher top speed and dynamicity than the WTLC.

The CADC150 and 3xUS06 chassis dyno tests at 23°C were performed with an AVL MOVE PEMS installed on the vehicles to verify the correct PEMS installation for the subsequent real-world driving tests and for assessing the accuracy of the PEMS-based fuel consumption calculation compared with the CVS analysis.

All tests were performed with type-approval reference fuel for which fuel composition analyses were available. The test conditions and number of tests performed with each vehicle are listed in Table 5. Tests with zero or very low fuel consumption, as encountered in the charge-depleting tests performed by the BMW X1 PHEV were excluded from the fuel consumption analysis. Tests with erroneous data were not considered.

Table 5. Overview of chassis dynamometer tests and test conditions. For each vehicle, the number of tests performed, the number of tests valid for deriving fuel consumption, and distance accuracy requirments are listed.

Cycle Type	Ambient temp. (°C)	A/C status (On/off) (°C)	Coolant at start	Number of tests: performed / valid FC data / valid distance data		
				Audi A3 (gasoline)	BMW X1 (gasoline)	Mercedes C-class (diesel)
WLTC	23	Off	Cold	3 / 3 / 3	CD: 2 / 0[a] / 1 CS: 1 / 1 / 1 CI: 1 / 1 / 1	2 / 2 / 2
WLTC	23	Off	Warm	1 / 1 / 1	CS: 2 / 0[b] / 1 CI: 1 / 1 / 1	1 / 1 / 1
WLTC	-5	On, 22	Cold	1 / 1 / 1	CD: 1 / 0[a] / 1	1 / 1 / 1
WLTC	-5	On, 22	Warm	-	CD: 1 / 0[a] / 1 CS: 2 / 2 / 2	-
WLTC	35	On, 22	Cold	1 / 1 / 1	CD: 2 / 0[a] / 2 CS: 1 / 1 / 1	1 / 1 / 1
WLTC	35	On, 22	Warm	-	CS: 1 / 1 / 1	-
3xNYCC	23	On, 22	Cold	1 / (1)[c] / (1)[c]	CS: 1 / (1)[c] / (1)[c]	1 / (1)[c] / (1)[c]
3xNYCC	-15	On, 22	Cold	1 / (1)[c] / (1)[c]	-	-
CADC150	23	On, 22	Cold	1 / 1 / 1	CS: 1 / 1 / 1	1 / 1 / 1
CADC150	-15	On, 22	Cold	1 / 1 / 1	-	-
3xUS 06	23	On, 22	Warm	1 /1 / 1	CS: 1 / 1 / 1	1 / 1 / 1
Total[d]				**11 / 9 / 9**	**18 / 9 / 15**	**8 / 7 / 7**

Notes: A/C: Air conditioning system, FC: Fuel consumption, CD: Charge-depleting mode, CS: Charge-sustaining mode, CI: Charge-increasing mode
[a] Charge-depleting mode tests where the engine was not or only very scarcely used were excluded from the fuel consumption analysis.
[b] Error between verification methods and CVS shows a large offset. Test considered as outlier.
[c] 3xNYCC test data is shown but not used for determining the OBFCM accuracy requirement recommendations.
[d] Only tests used for deriving OBFCM accuracy requirements are counted.

In addition to laboratory tests, tests were performed on public roads using two different routes. The route properties, the test conditions, and the number of tests performed with each vehicle are shown in Table 6. For these tests, the PEMS was installed in addition to the on-board verification measurement methods. Payload, driving style, and vehicle/transmission mode were varied for the tests, and both cold- and warm-start tests were performed to investigate a wide range of engine operating conditions. As for the chassis dyno tests, reference fuel of the same batch was used. Although not all tests are compliant with the RDE procedure requirements, we refer to them as RDE tests for simplicity. Sample speed trace and elevation profile for routes 1 and 2 are shown in Figure A1 in Appendix 1.

Table 6. Overview of valid RDE tests per vehicle

Route	Length [km]	Payload	Driving style	Number of tests / Coolant status / Ambient temperature		
				Audi A3 (gasoline)	BMW X1 (gasoline)	Mercedes C-Class (diesel)
1	87	Normal	Normal	1x warm (7°C) 1x cold (5°C)	1x warm (21°C) 2x cold (13–15°C)	2x warm (4–6°C) 1x cold (8°C)
		RDE Max	Dynamic	1x warm (10°C)	1x warm (18°C)	-
2	96	Normal	Normal	1x cold (4°C)	1x cold (12°C)	1x cold (6°C)
		RDE Max	Dynamic	-	1x warm (18°C)	-
Total				**4**	**6**	**4**

In addition to the RDE tests, data was also recorded when transferring the test vehicles. These tests were performed without PEMS and are referred to as vehicle transfer tests. For the vehicle transfer tests, mostly market fuel from public fuel stations was used.

2.4. RAW DATA PROCESSING METHOD FOR CYCLE FUEL CONSUMPTION AND DISTANCE VALUES

2.4.1. Fuel consumption

During type approval, volumetric fuel consumption is used to assess OBFCM accuracy. Following the same approach, we calculated the volumetric fuel consumption at a reference density of 15°C for each test and each verification method. For all chassis dynamometer and RDE tests, the test fuel properties from the supplier certificate were used in the calculations to minimize the effect of the fuel properties on the accuracy and to avoid introducing a bias error during conversion between volumetric and gravimetric fuel consumption.

The effect of fuel property variability when using market fuel on the achievable OBFCM accuracy is investigated separately, as described in section 2.7.1.

FFM. The fuel flow meter measures the instantaneous volumetric fuel flow intrinsically for the density at the current fuel temperature. The fuel flow rate is normalized to the reference temperature of 15°C using the instantaneous fuel density derived from the temperature-density slope (Wolf, 2015), which was adjusted to match the known test fuel density at 15°C.

Exhaust oxygen concentration and air mass flow. The volumetric fuel flow based on the exhaust oxygen concentration and air mass flow rate is calculated using the fuel density at reference temperature and the fuel composition—that is, the molar hydrogen-carbon ratio and oxygen-carbon ratio. We refer to the OBD signal-based verification method as $(O_2\text{+AFM})_{OBD}$ and the method using the tapped AFM signal and NO_x-sensor oxygen signal as $(O_2\text{+AFM})_{NOxS}$.

For the NO_x sensor used, the oxygen signal is not available for the first minutes of a test to allow for evaporation of water in the exhaust system to prevent sensor damage. Once activated, the sensor needs approximately 60 seconds to warm up. It was necessary to calculate fuel consumption for the entire cycle for comparison with the data from the CVS analysis and from OBFCM because both provide accumulated fuel consumption values but not second-by-second data. Therefore, we substituted the NO_x sensor-based volumetric fuel flow signal with the instantaneous OBD fuel flow signal until the NO_x sensor signal was available. This correction would be obsolete using latest-generation wideband oxygen sensors, which are more robustly designed and heat up in less than 7 seconds, but those were not available for this project. (Bosch, 2021)

PEMS. The PEMS measures the CO_2 and CO exhaust concentrations as well as the exhaust mass flow. To calculate the equivalent lambda value, the algorithm described in Silvis (1997) is used. In combination with the measured exhaust mass flow and the properties of the test fuel, the volumetric fuel flow is determined.

OBFCM. The OBFCM lifetime fuel consumption values were recorded every 10–20 seconds. The cycle fuel consumption was then calculated as the difference between the last and the first OBFCM value recorded for each test.

2.4.2. Distance

Chassis dynamometer. The vehicle speed signal on chassis dynamometer is equivalent to the measured rotational speed and known diameter of the solid chassis dynamometer rollers. By integrating this chassis dynamometer speed signal, the driven distance can be determined.

OBFCM. As with fuel consumption, the OBFCM lifetime distance value was recorded every 10–20 seconds. The distance driven was then calculated as the difference between the last and the first OBFCM value recorded in each test.

GPS distance. The GPS distance was calculated from the geolocation coordinates permanently measured by the DGPS device installed in the data logger. However, the following effects have a detrimental effect on the accuracy of the GPS position: the number and spatial distribution of satellites visible to the GPS receiver; signal reflections from surrounding buildings, mountains, and trees; and the connectivity to the DGPS reference station. To minimize the effect of these errors and to ensure comparability with the OBFCM distance values, we applied the following procedure:

In a first step, we smoothed the raw GPS latitude and longitude data with a moving average window filter of 1 second width to reduce signal noise.

Then, we calculated the discrete great-circle distances between each two adjacent GPS positions, from here on referred to as micro distance, using the haversine formula. Since the time difference between two datapoints is constant, the micro-distance signal is equivalent to the vehicle speed. We did not take into account the effect of slopes on the driven distance as it is less than 0.2% or negligible even for a mountainous road with a gradient of 6%.

Next, we performed a zero-speed drift correction to account for GPS position signal inaccuracy which could falsely indicate vehicle movement. To address this error source, we set the micro distance to zero whenever the OBD speed signal was zero. Beforehand, we time-aligned the GPS based and OBD speed signal using a cross-correlation function.

Before calculating the driven distance as the sum of the micro distances, we applied a correction for minimizing the effect of erroneous and missing GPS position records. While the GPS receiver records the number of visible and used satellites as well as the quality of the GPS fix, a comparison of these signals with GPS and OBD speed records revealed that a signal quality deterioration cannot be detected sufficiently this way. Instead, we calculated the difference between GPS and OBD vehicle speed signal and considered the GPS signal invalid whenever this gap exceeded 10 km/h. To ensure that also adjacent faulty data points are covered, we assumed the data recorded 2 seconds preceding and following each incident to be erroneous as well. For each time increment where the GPS speed signal was assumed to be faulty, it was replaced with the OBD speed signal. On average, 2.5% of the datapoints were replaced by this method for the RDE tests and 1.5% for the transfer tests.

2.4.3. Electric energy

OBFCM. In the case of the BMW X1 PHEV, the OBFCM grid energy consumption value was recorded every 10–20 seconds. The cycle energy consumption was calculated in the same way as the cycle fuel consumption and driven distance.

HVBM. The energy recharged to the battery as well as the energy consumption of electric motors and auxiliaries was calculated as the integrated power signal from the high voltage breakout modules.

2.5. METHODOLOGY APPLIED FOR COMPARING TWO MEASUREMENT METHODS

The core task of this project is the comparison of different methods of measuring the same parameter at the same time, called pairs of measurements. For this purpose, we used the methodology described by Bland & Altman (1999) and complemented by Carkeet (2015).

The Bland & Altman/Carkeet methodology determines the range where, for pairs of measurements, 95% of the differences between the measured values are expected. The limits defining the range are called the 95% limits of agreement (LoA_{95}). The upper and lower LoA_{95} are calculated as the mean of the differences, plus or minus 1.96 standard deviations. Instead of using the absolute difference, the relative difference can also be used. To account for the fact that both measurement methods compared are affected by measurement errors, the relative error is calculated as the absolute difference divided by the mean value of both methods. Providing the upper and lower LoA_{95} alone without determining their confidence interval disregards the fact that the analyzed sample presents only a subset of the infinite population of possible measurement value pairs. The method for determining the confidence interval applied by Bland & Altman is suited for large sample sizes. However, often only a few measurements can be made to draw conclusions on the agreement between two methods, as in our case. For this purpose, Carkeet presented a method to determine confidence intervals for the upper and lower LoA_{95} in case of small sample sizes, based on a noncentral t-distribution. The limits of agreement are considered as pairs, and therefore the same coefficients for defining the lower and upper boundaries of the confidence intervals are used for both lower and upper LoA_{95}.

We applied the described methodology to the accumulated fuel volume and distance values per test performed. This means that pairs of measurements are in this case the total fuel consumed, or total distance driven over a test, measured by two different methods.

2.6. ACCURACY ASSESSMENT OF VERIFICATION METHODS AND OBFCM DEVICES

Based on the cycle fuel consumption and driven distance determined according to section 2.4, and applying the methodology described in section 2.5, we analyzed the accuracy of the verification methods and of the OBFCM data as follows.[4]

4 Accuracy describes how close a measured value is to the “true” value. In this paper we use the term accuracy also to describe more generally how well two measurement methods correlate.

2.6.1. Fuel consumption

First, we evaluated how well the verification methods described in section 2.1 are suited for verifying OBFCM fuel consumption accuracy during real-world driving. As shown in Figure 1, we assessed the verification method accuracy on the chassis dynamometer by a comparison with the CVS bag analysis results.

For assessing the fuel consumption accuracy of the test vehicles' OBFCM devices on the chassis dynamometer, we compared the OBFCM value with the CVS data as well. For the tests performed on public roads, the OBFCM value was compared with the fuel consumption measured by the verification methods. To isolate the OBFCM device accuracy from any systematic error of the verification method, we corrected the values measured by the verification method by the mean error determined for each method on the chassis dynamometer when compared with CVS.

It should be noted that no correction was applied for the CO_2 generated from AdBlue injected in the Mercedes exhaust aftertreatment system, as neither the AdBlue consumption nor the NO_x emission reduction across the catalyst was measured[5]. AdBlue injection increases the CO_2 emissions measured by the CVS and the fuel consumption calculated therefrom by 0.3%–0.5%,[6] while the fuel consumption values determined by all other methods were not affected by the increased tailpipe CO_2 emissions.

Similarly, no correction was applied for the fuel introduced in the engine intake duct when purging the evaporative emission capturing systems of the Audi and BMW gasoline vehicle. It is unclear whether the OBFCM fuel consumption value takes the fuel coming from evaporative emission system into account, due to the ambiguous definition of the OBFCM parameter in the OBD standards (SAE J1979-DA, 2019) as the "amount of fuel injected into the engine", which does not specify whether fuel introduced in the intake duct from the evaporative system is considered as injected fuel. When assuming a carbon canister capacity of 1.02 g of fuel per liter fuel tank capacity, the canister load could be up to 46 g or 61 ml of gasoline E10 in case of the larger Audi tank (MECA, 2020). Burning this amount of fuel over one drive cycle would result in a total CO_2 mass of 140 g. However, since the vehicles were soaked and tested mostly at or below room temperature, only a low canister load at the start of each test is expected.

2.6.2. Distance driven

For determining OBFCM distance accuracy for the tests performed on the chassis dynamometer, the distance derived by integrating the chassis dynamometer speed signal is used as reference, which is expected to be very accurate considering the narrow speed tolerance of ±0.080 km/h required by the type-approval regulation (Regulation (EU) 2017/1151, 2017).

As reference value for assessing the OBFCM distance accuracy during real-world driving, the distance derived from the GPS signal as described in section 2.4.2 was used. To understand the accuracy of the GPS-based distance, we also derived the driven distance using Google maps, replicating the driven route from the recorded GPS coordinates.

We expect that the OBFCM distance determination is mainly based on the vehicle speed signal, calculated from the rotational speed of the wheels and the dynamic wheel radius. While the wheel speed is measured with a very high resolution and precision for feeding the electronic stability program (ESP) and antilock braking system (ABS), the dynamic wheel radius is presumably a calibrated parameter. The OBFCM distance accuracy might therefore be different on chassis dynamometer and

5 AdBlue is the trade name for an aqueous urea solution used in diesel exhaust aftertreatment systems for the reduction of NO_x emissions. In the United States it is commonly referred to as diesel exhaust fluid (DEF).

6 Assuming an AdBlue consumption of 3%–5% of the volumetric fuel consumption.

during on-road driving because a higher tire pressure is used on chassis dynamometer. This results in a larger dynamic wheel radius, and the patch between tire and the curved chassis dynamometer roller is smaller than between the tire and the flat road, which causes a reduction of the dynamic wheel radius. Which of the effects outweighs the other if any is unclear, so both higher and lower OBFCM accuracy seem possible. Furthermore, the higher tire pressure in combination with a smaller contact patch can lead to more tire slippage on the chassis dynamometer, especially in drive cycles with heavy accelerations. If not corrected by the vehicle electronics, the OBFCM would then determine a higher distance than the chassis dynamometer.

2.6.3. Electric energy consumption

For assessing the accuracy of PHEV-specific OBFCM parameters, the BMW X1 PHEV was equipped with HVBM electric power measurement devices for tracking the energy consumed and stored in the traction battery as described in section 2.2.3. The accuracy of the HVBM current measurement was verified during chassis dyno tests by comparison with a Hioki battery current clamp, which was installed as required by the PHEV type-approval provisions. Since the vehicle did not feature an access point for high-voltage measurement, the accuracy verification was limited to the current measurement. However, considering the high accuracy specifications of the HVBM voltage measurement, which would result in a measurement error of less than ±0.02% at the nominal system voltage of 295 V, the error in calculated power stemming from the voltage measurement is considered negligible (CSM GmbH, 2021).

The accuracy of the OBFCM recharged grid energy value, which is defined as the total grid energy charged to the battery excluding the on-board charger losses, was determined by comparison with the energy measured by the HVBM during battery charging.

2.6.4. Distance and fuel consumption in PHEV modes

OBD parameters including the OBFCM signals are defined in ISO 15031-5, which references the SAE standard SAE-J1979-DA (ISO, 2015). The SAE standard defines charge-depleting (CD) and charge-increasing (CI) mode as follows (SAE J1979-DA, 2019):

- **Charge-depleting mode:** The vehicle’s intent is depletion of the battery until charge sustaining state-of-charge (SoC) has been reached.
- **Charge-increasing mode:** The vehicle’s intent is to increase the battery SoC from its current level to a higher target value.

While this requirement describes in principle the two PHEV modes relevant for OBFCM data acquisition, the possibility of assessing the OBFCM accuracy in these modes is limited. This is because the target SoC is known only to the vehicle control unit, and an external instrument cannot determine directly whether the vehicle is in CD or CI mode. Furthermore, distance and fuel volume in the PHEV modes are provided only as accumulated lifetime values, not second-by-second, and it usually cannot be verified, for example, by comparison with the battery electric energy flow in which mode the vehicle is currently operating. However, since we polled the OBFCM lifetime values continuously and measured the battery energy flow with the HVBM, it was possible to estimate the present operating mode and thereby to analyze whether the fuel consumption and distance values were assigned to the correct OBFCM operating mode counter.

2.7. DETERMINATION OF HOW DIFFERENCES BETWEEN TYPE-APPROVAL AND REAL-WORLD OPERATION AFFECT OBFCM ACCURACY

Not all possible differences between type-approval and in-service verification that could affect OBFCM accuracy could be assessed through testing. Instead, a complementing theoretical analysis was performed as follows.

2.7.1. Effect on fuel consumption

When reference fuel is used, the density and composition of the fuel are known, and fuel mass, fuel volume, fuel energy, and exhaust carbon content can be directly converted without introducing errors. However, when testing a vehicle with market fuel, deviations in fuel properties from reference fuel affect the comparability of the OBFCM data with the values determined by the verification method. This is because the OBFCM is most likely calibrated for reference fuel. As it is unclear to what extent the engine control can determine the properties of the fuel currently in use, we investigated the potential effect of using market fuel on OBFCM fuel consumption accuracy.

For a quantitative analysis of the potential error, we purchased from SGS Germany GmbH a dataset of fuel properties stemming from market fuel samples of European gasoline E5 and E10 as well as diesel B7.[7] As shown in Table 7, the dataset covers a wide geographic range and contains samples taken in both summer and winter to address seasonal fuel variability. The interested reader can find how the fuel properties are distributed for the dataset in Figure A2 and Figure A3 of Appendix 3.

Samples of arctic diesel were excluded from the analysis as its usage in the European Union is geographically very limited. To improve the representativeness of the fuel properties derived from the SGS dataset for the European market, the number of probes taken in each country and the total fuel sales per country in 2019, derived from EEA (2021), were used for weighting the samples. In our analysis, we did not investigate the effect of using E85, which is used only in flex-fuel vehicles.

The equations used for assessing the potential error between OBFCM value and verification method measurement introduced by operating the vehicle on market fuel can be found in Table A1 of Appendix 2.

Table 7. Overview of fuel sample dataset composition

Fuel type	No. of countries	No. of samples taken Nov '19 – Feb '20	No. of samples taken May '20 – Aug '20	Analyzed fuel properties
Gasoline E5	10[a]	60	62	Density at 15°C; volumetric ethanol content; gravimetric carbon, hydrogen, and oxygen content
Gasoline E10	6[b]	32	31	
Diesel B7	11[c]	62	62	Density at 15°C; volumetric bio-diesel content

Notes: Fuel sample dataset was purchased from SGS Germany GmbH.
[a] Finland, France, Germany, Greece, Italy, the Netherlands, Poland, Spain, Sweden, United Kingdom.
[b] Bulgaria, Finland, France, Germany, the Netherlands, Romania.
[c] Bulgaria, France, Germany, Greece, Italy, the Netherlands, Poland, Romania, Spain, Sweden, United Kingdom.

7 Gasoline E5 and E10 and diesel B7 are standard fuels sold in the EU. E5 has an ethanol content of up to 5% and E10 up to 10% by volume. Diesel B7 can contain up to 7% biodiesel by volume. During EU type approval, gasoline E10 and diesel B7 are used.

2.7.2. Effect on distance measurement

As explained in section 2.6.2, OBFCM distance accuracy can be affected by uncertainties in dynamic wheel radius, which depends on tire dimension, tread wear, and pressure.

Tire dimensions. A vehicle can usually be fitted with tires of different width, height-to-width ratio, and rim diameter without requiring adjustments of the vehicle electronics, even though it can affect the dynamic rolling radius to some extent. For the three test vehicles, we investigated the effect of the approved tire dimension range on the accuracy of the distance measurement. To approximate the dynamic rolling radius depending on tire dimensions, Equation 1 was used. The dynamic radii calculated with this formula correlate well with the values stated in the Continental tire data book (Continental, 2020).

$$r_{dyn} = 0.97085 \times \left(w_{tire}\,[mm] \times \frac{hw_{ratio}\,[\%]}{100} + \frac{d_r\,[inch]}{2} \times 25.4 \right) \qquad \textbf{Equation 1}$$

With w_{tire} as the tire width in mm, hw_{ratio} as the height-to-width ratio in % and d_r as the rim diameter in inches.

Tire tread wear. Over a tire's lifetime, its radius changes due to tread wear. While a new tire has a profile depth of 8 mm–9 mm, the minimum tread depth legally allowed in the European Union is 1.6 mm. Many countries, however, require a minimum tread depth for winter tires of 3 mm–4 mm, the depths that also are recommended by automobile clubs (ADAC, 2021; AvD e.V., 2021a, 2021b). For analyzing the effect of tire tread wear on distance measurement accuracy, we assumed a maximum reduction of the dynamic radius due to tread wear of 5 mm over a tire's lifetime.

Tire pressure. Anghelache and Moisescu (2017) determined a linear dependency between tire pressure and dynamic radius. When reducing tire inflation pressure by 46%, a dynamic radius reduction of about 0.9% was observed, independent of vehicle speed. The ratio of change in dynamic radius relative to the pressure reduction is therefore approximately 0.02.

To estimate the tire pressure range to be expected in real-world operation, it needs to be considered that category M1 vehicles are equipped with tire pressure monitoring systems (TPMS), which are compulsory in the European Union for all new vehicles. Regulation (EC) 661/2009 requires TPMS to detect a tire pressure loss of 20% in one wheel within 10 minutes of driving and a loss of the same magnitude in one or more wheels within 60 minutes. (EC 661/2009, 2009; UNECE R141 Add 140, 2017).

It can therefore be assumed that the largest change in tire pressure that could remain unnoticed by the vehicle is 20%, which needs to be considered in the distance measurement accuracy assessment. Applying the radius-change to pressure-change ratio of 0.02, the maximum unnoticed change in dynamic radius due to pressure is expected to be about 0.4%.

2.8. DERIVATION OF COMBINED OBFCM ACCURACY REQUIREMENT RECOMMENDATIONS

When determining OBFCM accuracy recommendations for verification tests on chassis dynamometer or on public roads, the individual uncertainties of the OBFCM device, the verification method, and the effects of market fuel and tire variability need to be considered, where applicable. We calculated the total OBFCM uncertainty by applying standard error propagation mechanisms for multiplicative dependencies as described for example in Fantner (2013). More details are available in Appendix 4.

3. DATA ANALYSIS AND CONCLUSIONS

By applying the methodologies presented in section 2, we performed the following analyses:

» Based on the test data, we assessed the accuracy of the verification methods for fuel consumption and distance driven to be used during real-world driving.

» We analyzed the accuracy of the test vehicles' OBFCM devices both on chassis dynamometer and during real-world driving.

» We determined theoretically how much the OBFCM fuel consumption and distance accuracy can be affected by deviations from type-approval reference conditions not investigated as part of the test program.

» Finally, we derived recommendations for OBFCM fuel and distance accuracy requirements separately for chassis dynamometer and real-world testing.

3.1. VOLUMETRIC FUEL CONSUMPTION DETERMINATION

3.1.1. Accuracy of the fuel consumption verification methods

Test results

For assessing how suitable the methods presented in section 2.1 are for verifying OBFCM fuel consumption accuracy during real-world driving, we first analyzed the accuracy of each method on the chassis dynamometer in comparison with the CVS bag analysis, which is the methodology used for determining fuel consumption during type approval. As explained in section 2.3, the 3xNYCC tests were excluded from the analysis. Two WLTC tests performed with the BMW at 23°C were considered outliers because the errors determined for those tests were much larger than for similar WLTC tests performed with the same vehicle.

Based on the relative errors calculated for each test, vehicle, and verification method we then determined the 95% level of agreement and the 95% confidence interval for the upper and lower LoA_{95} limit, as described in section 2.5. The results are presented in Figure 3, and the data values are listed in Table 8. A positive error represents the case where the verification method measures a higher value than the CVS and vice versa for a negative error. The BMW outlier tests are reflected by cross markers. For the Audi, the salient FFM and $(O_2\text{+AFM})_{OBD}$ datapoints show the error of the WLTC test performed at -5°C. Even though we expect those results are outliers, we include them in the following analysis as no fault could be detected in the test data.

Figure A4 in Appendix 5 shows the absolute fuel consumption values measured by the different methods.

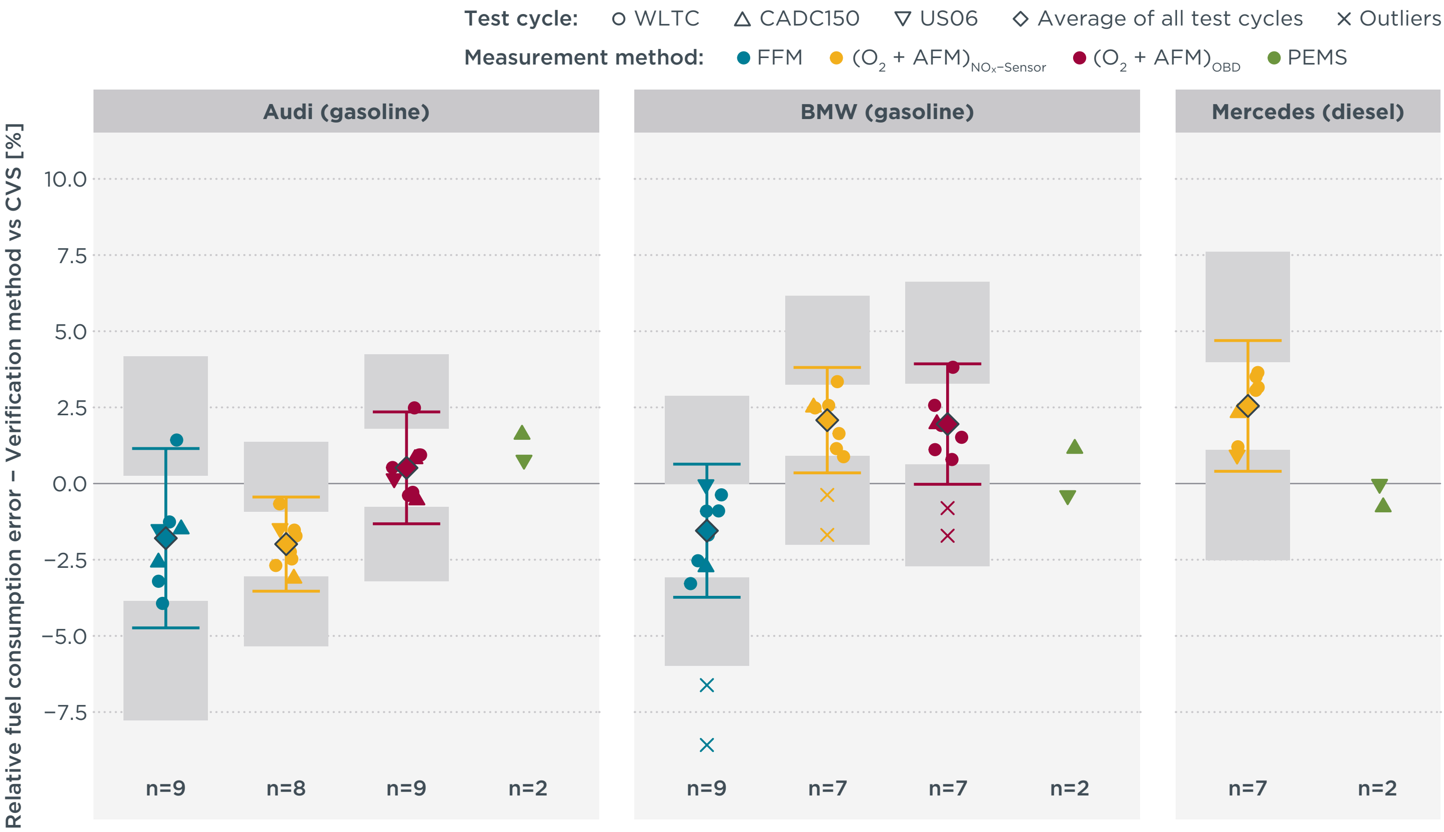

Figure 3. Fuel consumption error between verification method and CVS for tests performed on chassis dynamometer. The error bars show the upper and lower limit of the 95% level of agreement while the grey shaded rectangles indicate the 95% confidence interval of the upper and lower limit. The data shown includes all valid tests at -15°C, -5°C, 23°C, and 35°C according to Table 5 in section 2.3, except for the 3xNYCC tests.

The FFM tested in the Audi underestimates the fuel consumption on average by -1.8% and in the BMW by -1.6%. The spread of results around the mean error, indicated by the LoA_{95} range, is ±2.2% for the BMW, much smaller than the ±2.9% determined for the Audi. For the diesel Mercedes, no FFM data is available as explained in section 2.1.3.

The mean error of the NO_x-sensor based $(O_2+AFM)_{NOxS}$ method varies from vehicle to vehicle. While it is -2.0% for the Audi, the $(O_2+AFM)_{NOxS}$ method overestimates the fuel consumption by 2.1% for the BMW and 2.6% for the Mercedes. The LoA_{95} range observed on the diesel Mercedes vehicle is ±2.2% around the mean, larger than the similar spreads of ±1.6% for the Audi and ±1.7% for the BMW. This observation is expected, considering that the mixture-quality controlled diesel combustion entails a very transient air-fuel ratio, and thus exhaust oxygen concentration fluctuations, whereas the stoichiometric BMW and Audi gasoline engines operate at an almost constant air-fuel ratio, reducing the potential error stemming from the oxygen signal.

Only the Audi and the BMW broadcast the relevant OBD signals for calculating the $(O_2+AFM)_{OBD}$ fuel consumption value. The mean error on the BMW is 2.0% while the Audi's error is only 0.5%. The LoA_{95} range of the $(O_2+AFM)_{OBD}$ method for the BMW distributes by ±2.0% around the mean, similar to the $(O_2+AFM)_{NOxS}$ method and FFM on the same vehicle. On the Audi, the LoA_{95} range of the $(O_2+AFM)_{OBD}$ method shows a similar spread of ±1.8 percentage points around the mean.

No LoA_{95} range and confidence interval were calculated for the PEMS measurements as only two tests were performed on each vehicle. Nevertheless, for the tests performed, the mean error between PEMS-based fuel consumption and CVS was about 1.2% on the Audi, 0.4% on the BMW and -0.4% on the Mercedes.

Table 8. Overview of mean error, 95% level of agreement (LoA_{95}) and the LoA_{95}'s respective 95% confidence interval for four fuel consumption verification methods compared with CVS bag analysis, aggregated per vehicle.

Vehicle	Verification method	No. of tests	Mean ± ½ LoA_{95} range [%]	LoA_{95} 95% confidence interval	
				Inner [%]	Outer [%]
Audi	FFM	9	-1.79 ±2.94	0.89	3.03
BMW	FFM	9	-1.55 ±2.19	0.66	2.25
Audi	$(O_2\text{+AFM})_{NOxS}$	8	-1.99 ±1.55	0.48	1.80
BMW	$(O_2\text{+AFM})_{NOxS}$	7	2.08 ±1.73	0.57	2.35
Mercedes	$(O_2\text{+AFM})_{NOxS}$	7	2.55 ±2.15	0.70	2.92
Audi	$(O2\text{+AFM})_{OBD}$	9	0.52 ±1.84	0.55	1.89
BMW	$(O_2\text{+AFM})_{OBD}$	7	1.95 ±1.98	0.65	2.69
Audi	PEMS	2	1.19	N/A	N/A
BMW	PEMS	2	0.38	N/A	N/A
Mercedes	PEMS	2	-0.39	N/A	N/A

To assess the accuracy of the verification methods across vehicles, we calculated the LoA_{95} and confidence interval for each method for all vehicles combined, mimicking the scenario that all tests were performed on the same vehicle. The results are shown in Figure 4 and Table 9. To separate the random error from the systematic errors observed, the mean error of each method on each vehicle was subtracted from the individual errors of each measurement. Since PEMS and FFM are vehicle and calibration-independent methods, the mean error across all vehicles was calculated, listed in Table 9. For the vehicle-dependent (O_2+AFM) methods (refer to section 2.2.2) calculating a mean error across the vehicles would not be meaningful.

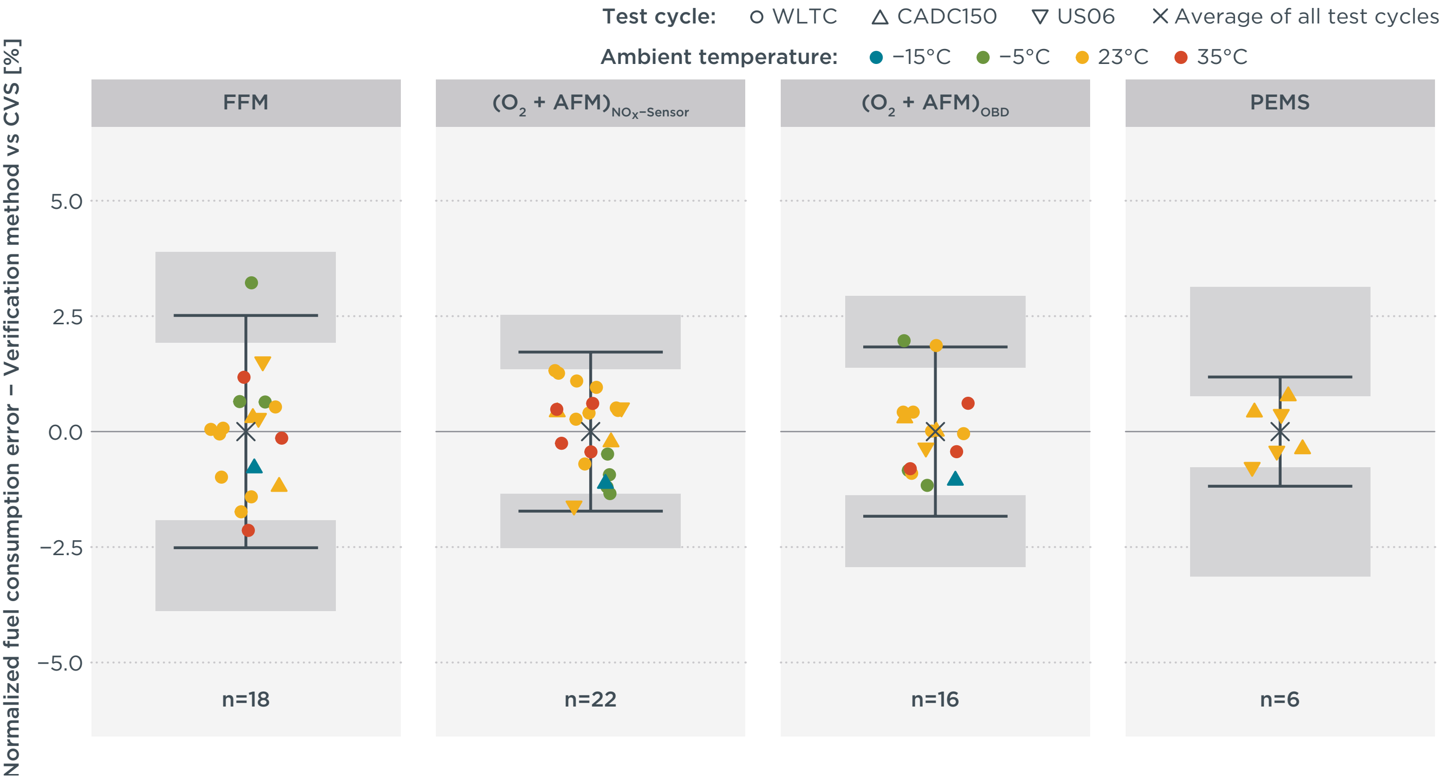

Figure 4. Precision of fuel consumption verification methods across all vehicles when compared with CVS. The individual test results are normalized by subtracting the mean error of each method and vehicle. The error bars show the upper and lower limit of the 95% level of agreement while the grey shaded rectangles indicate the 95% confidence interval of the upper and lower limit. The 3xNYCC tests as well as outlier tests are excluded.

The mean FFM error across all vehicles is -1.7%, and the LoA_{95} spreads about ±2.5 percentage points around this mean. The $(O_2+AFM)_{NOxS}$ method has a narrower LoA_{95} spread than the FFM of ±1.7, and the $(O_2+AFM)_{OBD}$ has a spread of ±1.8. For the PEMS, the LoA_{95} range is even smaller with ±1.2 percentage points around the mean error of 0.4%. However, the PEMS results are only comparable with some limitation, as measurements were performed only during the 3xUS06 and CADC150 tests at 23°C.

Table 9. Summary of error between verification method and CVS, aggregated per method and across all vehicles.

Method	No. of tests	Mean [%]	½ LoA_{95} range [%]	LoA_{95} 95% confidence interval	
				Inner [%]	Outer [%]
FFM	18	-1.67	±2.51	0.59	1.37
$(O_2+AFM)_{NOxS}$	22	N/A*	±1.72	0.38	0.80
$(O_2+AFM)_{OBD}$	16	N/A*	±1.83	0.45	1.10
PEMS	6	0.39	±1.18	0.41	1.95

*Method not independent of vehicle. Meaningful mean error for aggregation across vehicles cannot be calculated.

Conclusion

The test results indicate that all methods investigated are suited for verifying the OBFCM fuel consumption with sufficient accuracy during real-world tests. For the vehicle-independent FFM, we expect that the systematic error can be largely eliminated in a series product. It should also be noted that the large LoA_{95} spread of the FFM is strongly influenced by the one -5°C WLTC test performed with the Audi, presumably being an outlier. When excluding this test from the analysis, the LoA_{95} range decreases to ±2.0%.

Both (O_2+AFM) methods have good precision even for the more challenging drive cycles and extreme ambient conditions, indicated by a narrow LoA_{95} range. We assume that the systematic error observed for these methods is related to the transfer curve used for the AFM signal, and in the case of the OBD air flow signal, the low time resolution of only 1 Hz. Therefore, when using fast-responding, latest-generation exhaust oxygen sensors and vehicle-independent air- or exhaust-mass-flow meters, we expect that the systematic errors observed for the (O_2+AFM) methods can be abated and precision further improved. Without the Audi WLTC test at -5°C, the LoA_{95} range of the $(O_2+AFM)_{OBD}$ method drops from above ±1.8 to less than ±1.6%, while it remains at ±1.7% for the $(O_2+AFM)_{NOxS}$ method.

Also, the PEMS showed very good agreement with the CVS measurements on all three vehicles, although for a lower number of tests performed.

Based on our analysis, we expect that the uncertainty of the fuel consumption verification method will be within ±2.5% when verifying real-world OBFCM fuel consumption accuracy. This range comprises the LoA_{95} ranges of both (O_2+AFM) methods as well as of PEMS and the pre-series FFMs. For all methods investigated, we therefore expect that the range of ±2.5% contains a sufficient margin for any device-to-device variability, especially when considering that the LoA_{95} even of the current FFM is most likely closer to ±2.0% than ±2.5%, as explained above.

3.1.2. The accuracy of the test vehicles' OBFCM devices

The accuracy of the OBFCM fuel consumption determination was analyzed separately for chassis dynamometer and real-world driving tests.

Test results for OBFCM accuracy on chassis dynamometer

During type approval, manufacturers need to demonstrate in a cold-started WLTC performed at 23°C that the volumetric fuel consumption determined by the OBFCM deviates by less than 5% from the CVS value. When replicating a WLTC under these conditions, both Audi and Mercedes were well within the regulatory limits, as presented in Figure 5. The BMW also met the regulation requirement, though being very close to the upper limit, meaning the vehicle overestimates true fuel consumption by almost 5%.

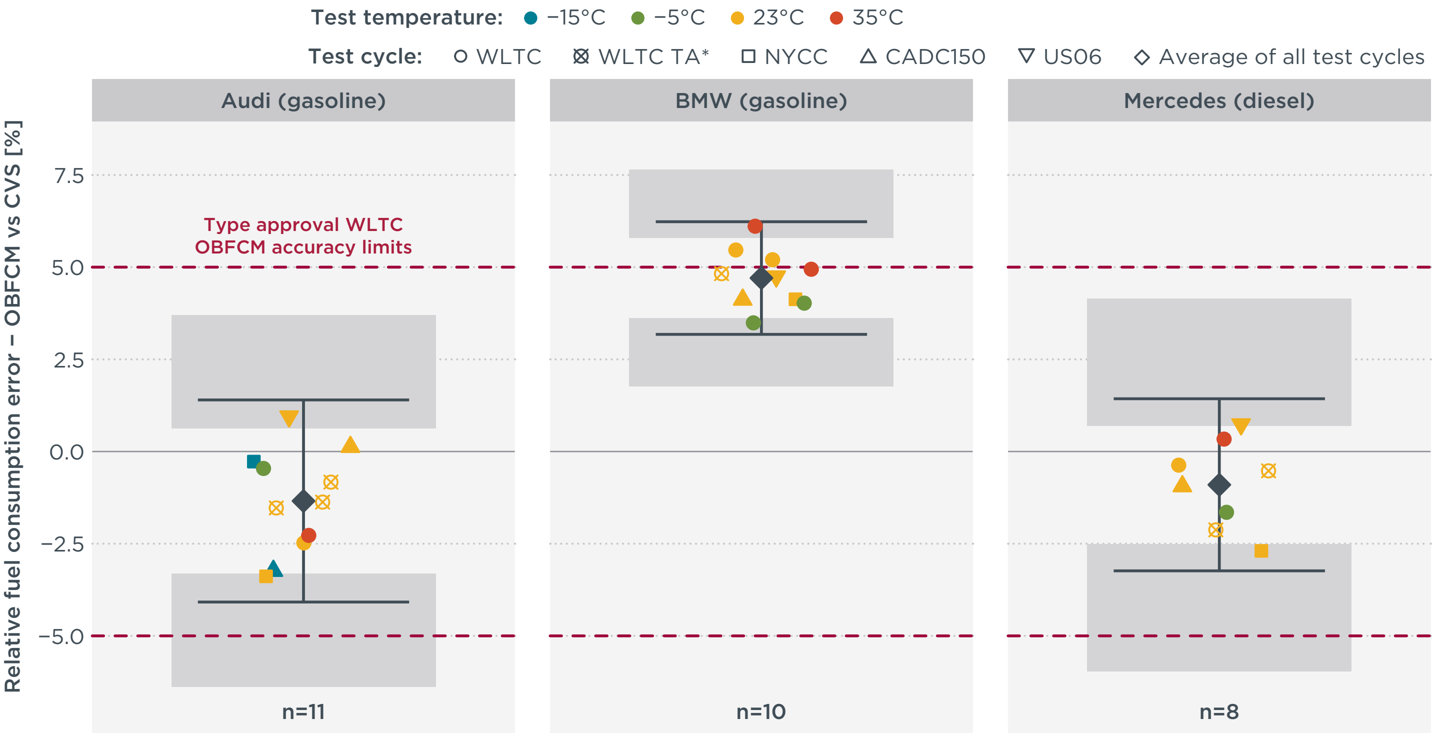

Figure 5. Relative error between OBFCM and CVS fuel consumption based on all valid tests performed on chassis dynamometer. For each vehicle, the error for each test as well as the mean error of all tests are shown together with the 95% level of agreement (error bars) and the 95% confidence intervals of the upper and lower limit of the level of agreement (grey areas). *Test under type-approval conditions (23°C, cold started). In charge-sustaining mode for the BMW PHEV.

A similar observation can be made for the other drive cycles with a more demanding speed profile or at more extreme ambient conditions. For all of these tests, the OBFCM error of both Audi and Mercedes remains well within the ±5% limit, as shown in Figure 5. Again, the BMW OBFCM shows a large offset toward overestimating fuel consumption, exceeding the limit in three tests, two of them being WLTCs at 23°C in charge-increasing mode.

Table 10 contains the statistical parameters of the test results presented in Figure 5, including tests at extreme ambient conditions, the short and low-load 3xNYCC, and the high-load and high-speed CADC150 and 3xUS06.

Table 10. Summary of OBFCM fuel consumption accuracy compared with CVS on chassis dynamometer for all valid tests performed, including the 3xNYCC tests.

Vehicle	No. of tests	Mean ± ½ LoA_{95} range [%]	LoA_{95} 95% confidence interval	
			Inner [%]	Outer [%]
Audi	11	-1.34 ±2.74	0.77	2.31
BMW	10	4.70 ±1.53	0.44	1.41
Mercedes	8	-0.90 ±2.33	0.73	2.72

While the BMW OBFCM notably overestimates fuel consumption on average by about 4.7%, the Audi and Mercedes OBFCMs underestimate it by 1.3% and 0.9% respectively. At the same time, the BMW has the smallest spread of the LoA_{95} of only ±1.5 percentage points around the mean error, showing that the precision of the BMW OBFCM device is very good. The Mercedes LoA_{95}-range is ±2.3% while it is ±2.7% for the Audi, and thereby almost twice as large as for the BMW. It should be noted that the large mean error observed on the BMW is in principle to the disadvantage of the manufacturer, while the offsets observed on the Audi and Mercedes would lead to an underestimation of real-world fuel consumption, constituting an advantage for these manufacturers when determining the real-world to type-approval fuel consumption gap.

For determining the fuel consumption accuracy that can reasonably be required of OBFCM devices when verified on chassis dynamometer, we included only a subset of the tests in the analysis. Assuming that the verification will be performed for WLTC tests at type-approval conditions, we considered only tests performed at 23°C ambient temperature and excluded the 3xNYCC and 3xUS06 tests for having more severe conditions for fuel consumption determination than the WLTC speed profile (refer to section 2.3). To limit the effect of test-to-test variability, we included the CADC150 drive cycles in the analysis, even though the maximum speed and dynamicity are higher than for the WLTC and thereby might exceed the operating range for which the OBFCMs were calibrated.

Since there is no compelling technical reason for a systematic OBFCM fuel consumption error, except for the ones addressed separately in section 3.1.3, we expect that the OBFCM offset observed on all three vehicles can be largely eliminated by the manufacturers through improved calibration. Therefore, we determined the OBFCM precision for each vehicle after normalizing the individual errors by subtracting the mean error of all tests, shown in Figure 6 and summarized in Table 11. The table shows also in the rightmost column the LoA_{95} for the case that all valid chassis dynamometer tests are considered.

Table 11. Relative error between OBFCM and CVS fuel consumption based on all valid WLTC and CAD150 tests performed at 23°C and compared with the results when considering all valid tests performed at all ambient conditions.

Vehicle	Only tests at 23°C, excluding 3xNYCC and 3xUS06				All valid tests	
	No. of tests	± ½ LoA_{95} range [%]	LoA_{95} 95% conf. interval		No. of tests	± ½ LoA_{95} range [%]
			Inner [%]	Outer [%]		
Audi	5	±1.88	0.69	4.02	11	±2.74
BMW	4	±1.15	0.46	3.61	10	±1.53
Mercedes	4	±1.55	0.62	4.87	8	±2.33
Weighted mean	-	**±1.55**	-	-	-	**±2.21**

The results show that OBFCMs of today's vehicles on chassis dynamometer under type-approval conditions have much better precision—between ±1.2 and ±1.9%—than the regulatory requirement of ±5%. Even when including the tests at extreme ambient conditions as well as the more severe 3xNYCC and 3xUS06 drive cycles in the analysis, the weighted average accuracy is ±2.2%, or more than twice as accurate as the regulatory limit.

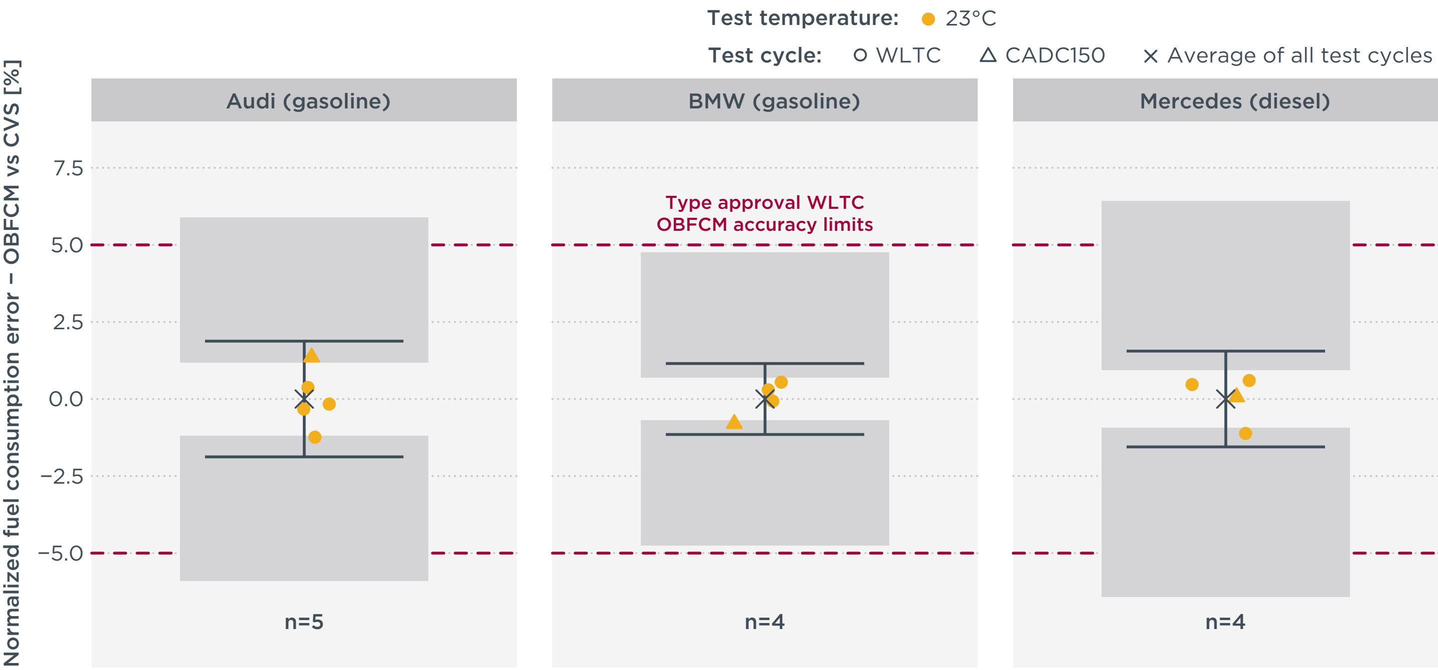

Figure 6. Relative error between OBFCM and CVS fuel consumption based on all valid WLTC and CADC150 tests performed at 23°C. The errors are normalized by subtracting the mean error from the individual test errors. The error bars show the upper and lower limit of the 95% level of agreement while the grey shaded rectangles indicate the 95% confidence interval of the upper and lower limit.

Test results for OBFCM accuracy during real-world driving

For assessing OBFCM accuracy during RDE tests and real-world driving, we compared the OBFCM fuel consumption with the values measured by the different verification methods. To separate OBFCM accuracy from the effect of the verification method error, we subtracted for each verification method the mean error determined on chassis dynamometer, as described in section 3.1.1, from the error of the respective method calculated for each real-world driving test.

Figure 7 and Table 12 show the relative error between OBFCM fuel consumption and the value measured by the verification methods during RDE tests and other real-world driving for the three tested vehicles.

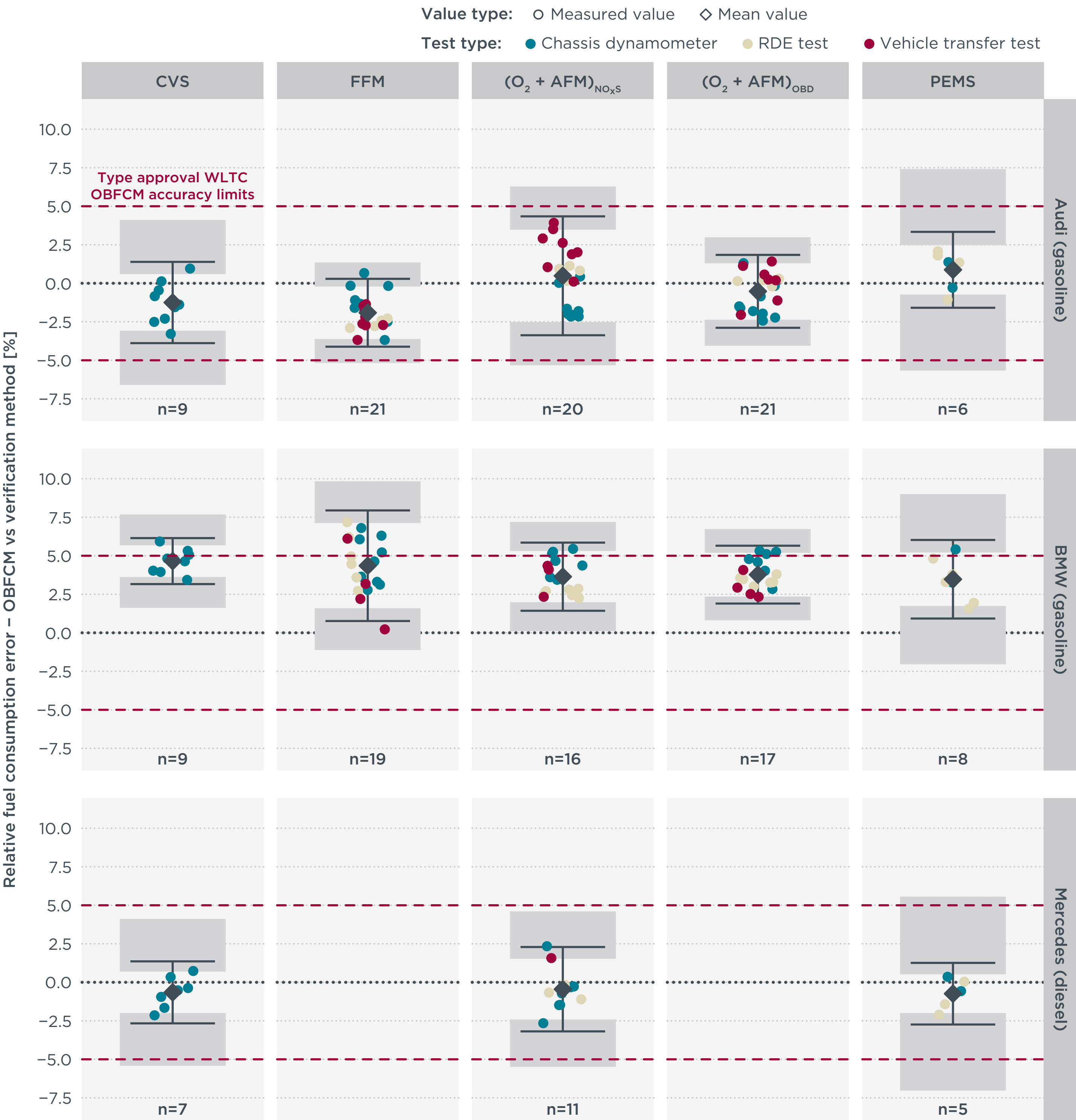

Figure 7. OBFCM fuel consumption error per vehicle when compared with the different verification methods available, corrected for the average error between verification method and CVS determined on chassis dynamometer. Each column shows per verification method the individual results of chassis dynamometer, RDE and vehicle transfer tests and the mean error of all tests. The chassis dynamometer results include the data of all valid tests except for the 3xNYCC. The error bars show the upper and lower limit of the 95% level of agreement while the grey shaded rectangles indicate the 95% confidence interval of the upper and lower limit.

For comparability, the chassis dynamometer tests and the comparison with the CVS were also contained. To reflect that real-world tests can be performed under a wide range of ambient conditions and driving patterns, we included for better comparability the chassis dynamometer results of the 3xUS06 tests as well as the tests performed at extreme ambient temperatures in this comparison. It should be noted that all chassis dynamometer and RDE tests were performed with reference fuel with known composition while vehicle transfer was mostly performed using market fuel from public gas stations. Furthermore, the BMW RDE test results had to be corrected for a presumably faulty PEMS exhaust-flow meter signal during these tests. More details about this correction can be found in Appendix 6.

Table 12. Average OBFCM fuel consumption accuracy on chassis dynamometer, during RDE and vehicle transfer tests relative to CVS and four on-board verification methods.

Vehicle	Measurement method	No. of tests[a]	Mean ± ½ LoA_{95} range [%]	LoA_{95} 95% confidence interval	
				Inner [%]	Outer [%]
Audi	CVS[b]	9	-1.25 ±2.64	0.79	2.71
Audi	$(O_2+AFM)_{NOxS}$	20	0.48 ±3.86	0.87	1.94
Audi	$(O_2+AFM)_{OBD}$	21	-0.52 ±2.37	0.52	1.14
Audi	FFM	21	-1.91 ±2.20	0.49	1.07
Audi	PEMS[c]	6	0.87 ±2.46	0.85	4.07
BMW	CVS[b]	9	4.66 ±1.49	0.45	1.54
BMW	$(O_2+AFM)_{NoxS}$	16	3.64 ±2.21	0.54	1.33
BMW	$(O_2+AFM)_{OBD}$	17	3.78 ±1.88	0.45	1.07
BMW	FFM	19	4.35 ±3.59	0.83	1.88
BMW	PEMS[c]	8	3.47 ±2.55	0.80	2.98
Mercedes	CVS[b]	7	-0.65 ±2.01	0.66	2.74
Mercedes	$(O_2+AFM)_{NoxS}$	11	-0.45 ±2.74	0.77	2.31
Mercedes	PEMS[c]	5	-0.74 ±2.00	0.74	4.28

Notes: For analyzing the OBFCM accuracy, the values measured by the verification methods were adjusted for the vehicle-specific mean error of each verification method determined on chassis dynamometer.
[a] Valid tests, except the 3xNYCC tests.
[b] Method available only for tests performed on chassis dynamometer.
[c] On chassis dynamometer, only two tests at 23°C were performed.

The Audi results show a similar spread of the LoA_{95} range around the mean error between 2.2% (FFM) and 2.6% (CVS) for all verification methods except for the $(O_2+AFM)_{NOxS}$ method, where the spread is almost ±3.9%. For FFM, PEMS and $(O_2+AFM)_{OBD}$, the errors are also largely randomly distributed within the LoA_{95} ranges. We therefore assume that the noticeable shift of the $(O_2+AFM)_{NOxS}$ error, observed for the Audi when comparing the chassis dynamometer tests with the RDE and vehicle transfer tests, stems from the $(O_2+AFM)_{NOxS}$ fuel consumption measurement and is not attributed to a change in OBFCM accuracy. This shift also causes the much larger LoA_{95} range. Overall, we conclude that the Audi OBFCM accuracy does not deteriorate when switching from controlled laboratory conditions to real-world driving.

The same conclusion can be drawn for the BMW OBFCM. The mean fuel consumption error is very similar for all verification methods and confirms the overestimation of the OBFCM measurement observed on chassis dynamometer also when driving on public roads. The mean error ranges from 3.5% in the case of the PEMS to 4.4% for the FFM. When comparing the OBFCM fuel consumption with findings of other methods, similar mean OBFCM errors of 3.6% for $(O_2+AFM)_{NOxS}$ and 3.8% for $(O_2+AFM)_{OBD}$ appear. The LoA_{95} spread around the mean is ±2.2% determined for the $(O_2+AFM)_{NOxS}$ method, which is slightly larger than the ±1.9% for the $(O_2+AFM)_{OBD}$ method and lower than the ±2.6% for PEMS. Unexpectedly, the OBFCM error when compared with the FFM shows a relatively large LoA_{95} spread of ±3.6%. The fact that the correlation between OBFCM and FFM is much better on the Audi, indicated by the substantially narrower LoA_{95} range, suggests that the installation of the FFM in the Audi close to the fuel tank is preferable compared with the engine close-coupled installation in the BMW.

On the Mercedes, only the $(O_2+AFM)_{NOxS}$ method and PEMS are available for comparison with the OBFCM fuel consumption as explained in section 2.4. The random distribution of the error when compared with both the $(O_2+AFM)_{NOxS}$ method and PEMS indicates that OBFCM accuracy for the Mercedes is not affected by switching from chassis dynamometer to testing on public roads. The mean OBFCM error is similar for all methods, ranging from -0.5% for the $(O_2+AFM)_{NOxS}$ method to -0.7% for the PEMS and CVS. The LoA_{95} range spreads by ±2.0 percentage points around the mean in case of the CVS and PEMS and by ±2.7% for the comparison with the $(O_2+AFM)_{NOxS}$ method.

As previously noted, we assume that systematic OBFCM errors can largely be eliminated. The uncertainty of the verification method, determined in section 3.1.1, will be considered separately when determining the combined OBFCM accuracy requirement recommendations. Figure 8 shows the normalized OBFCM errors after subtracting the mean error, determined per vehicle and verification method. In each column, the normalized errors determined for all valid chassis dynamometer, RDE, and vehicle transfer tests performed with the three vehicles are shown per verifcation method. The same information is summarized in Table 13. This analysis shows that when considering chassis dynamometer tests at extreme ambient conditions and more-severe drive cycles, the OBFCM precision for chassis dynamometer testing, indicated by the CVS column, and real-world driving is similar and largely independent of the verification method.

Table 13. Normalized, relative OBFCM fuel consumption error when compared with the different verification methods, aggregated per verification method for all vehicles.

Verification method	No. of tests	± ½ LoA_{95} range [%]	LoA_{95} 95% conf. interval	
			Inner [%]	Outer [%]
CVS	25	±2.02	0.42	0.85
FFM	40	±2.90	0.50	0.88
$(O_2+AFM)_{NOxS}$	47	±3.06	0.50	0.83
$(O_2+AFM)_{OBD}$	38	±2.13	0.38	0.67
PEMS	19	±2.26	0.52	1.18

Notes: For determining the individual OBFCM errors, the values measured by the verification methods were adjusted for the mean error determined on chassis dynamometer. The chassis dynamometer results include the data of all valid tests except for the 3xNYCC.

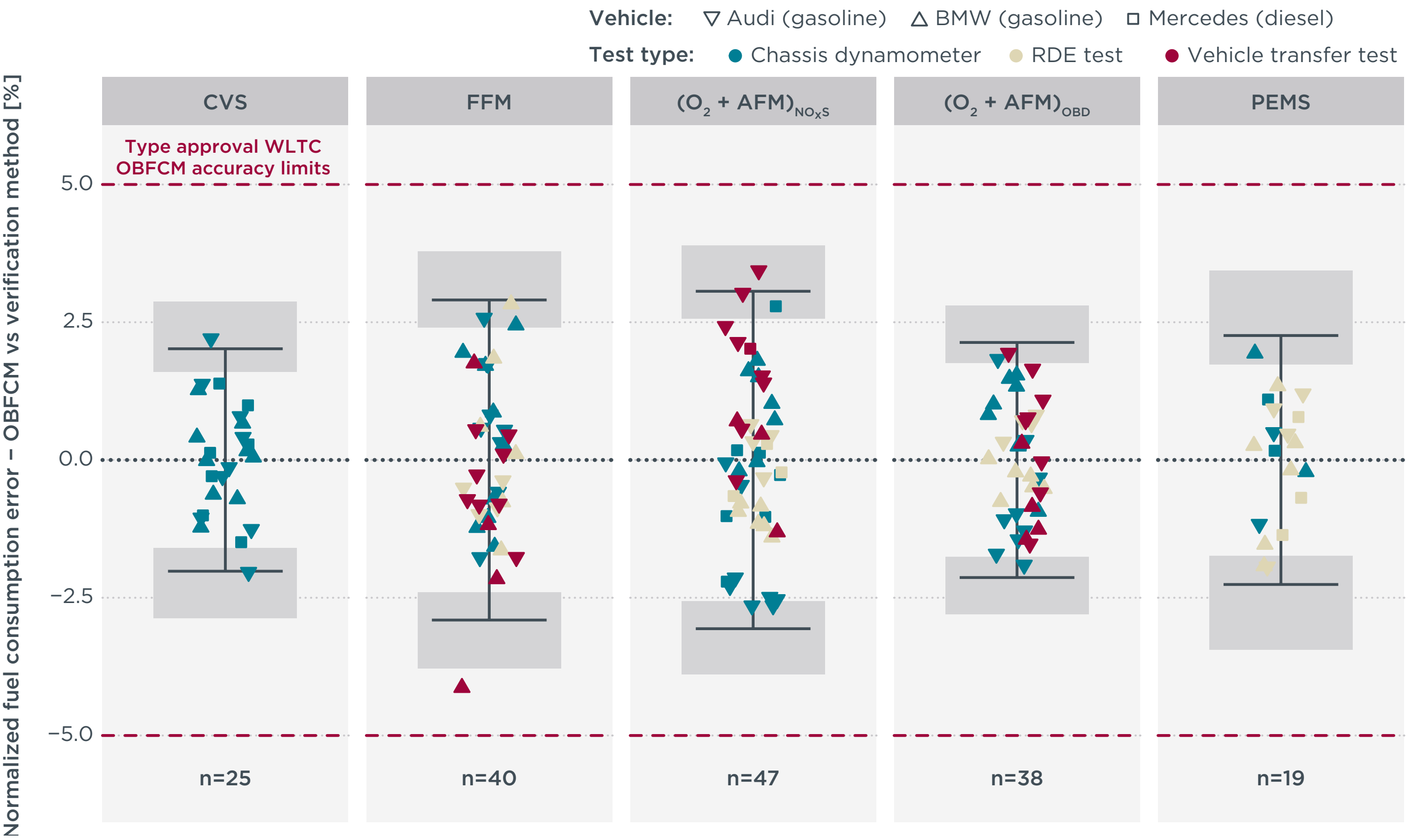

Figure 8. Normalized, relative OBFCM fuel consumption error when compared with the different verification methods (columns). The individual test errors are normalized by subtracting the mean error per vehicle and verification method. The chassis dynamometer results include the data of all valid tests except for the 3xNYCC. The error bars show the upper and lower limit of the 95% level of agreement while the grey shaded rectangles indicate the 95% confidence interval of the upper and lower limit.

Conclusion

The accuracy of OBFCM fuel consumption determined on chassis dynamometer at conditions similar to type approval for today's vehicles is already much better than the applicable ±5% regulatory limit. It is therefore justified to apply tighter OBFCM fuel consumption accuracy limits for chassis dynamometer testing. We suggest using the weighted mean LoA_{95} range of all vehicles of ±1.55% as a revised accuracy requirement for WLTC tests performed on chassis dynamometer at type-approval conditions with reference fuel. While this seems to disregard any effect of vehicle-to-vehicle variability on the OBFCM error, it should be considered that the OBFCM devices of the tested vehicles were developed only for meeting the current requirements. We therefore expect that higher OBFCM fuel consumption precision is possible, compensating for the vehicle-to-vehicle variability.

When comparing the OBFCM fuel consumption error for real-world tests with tests performed on chassis dynamometer, it becomes apparent that no OBFCM accuracy deterioration is to be expected for real-world driving except for the effects of a wider range of dynamicity or ambient conditions. On this basis, we consider the precision of the OBFCM devices when compared with CVS or $(O_2\text{+AFM})_{OBD}$ of about ±2.1% as a reasonable accuracy requirement for OBFCM devices during real-world testing using reference fuel. Choosing this value is also justified because most of the vehicle transfer tests were peformed using market fuel instead of reference fuel, for which an extra uncertainty will be considered when determining combined OBFCM accuracy requirements, as discussed in the next section.

3.1.3. Effect of market fuel composition variability on OBFCM accuracy

Since some type-approval and in-service verification tests can be performed with market fuel, we investigated how deviations from reference fuel can affect OBFCM accuracy, if not compensated for with engine control, as described in section 2.7.1.

Figure 9 shows the distribution of OBFCM-versus-verification-method error separately for diesel and gasoline market fuel properties as well as the 68% confidence interval (1-sigma) around the mean error. Each column represents a case where the OBFCM measurement methodology, labeled "OM," differs from the methodology applied by the verification method, marked as "VM." The cases where the OBFCM and verification measurement method are interchanged, the results are mirrored at the 0-error line. For a better overview, this is not shown in the figure but only in Table 14. It should be noted that measurement of fuel energy by verification method was not considered as no such method is known.

A 1-sigma confidence interval was chosen to account for the fact that for tests where market fuel is often used—the in-service conformity and market surveillance tests—multiple vehicles are usually tested to arrive at a compliance decision. Testing multiple vehicles reduces the effect of market fuel variability. Instead of diluting the accuracy requirements to cover niche market fuel compositions, we recommend that a fuel sample analysis be conducted in case a vehicle fails a verification test and the fuel properties are assumed to be the cause. We further expect that controls of modern combustion engines can at least partly detect and compensate for fuel composition variability, which is not accounted for in our analysis.

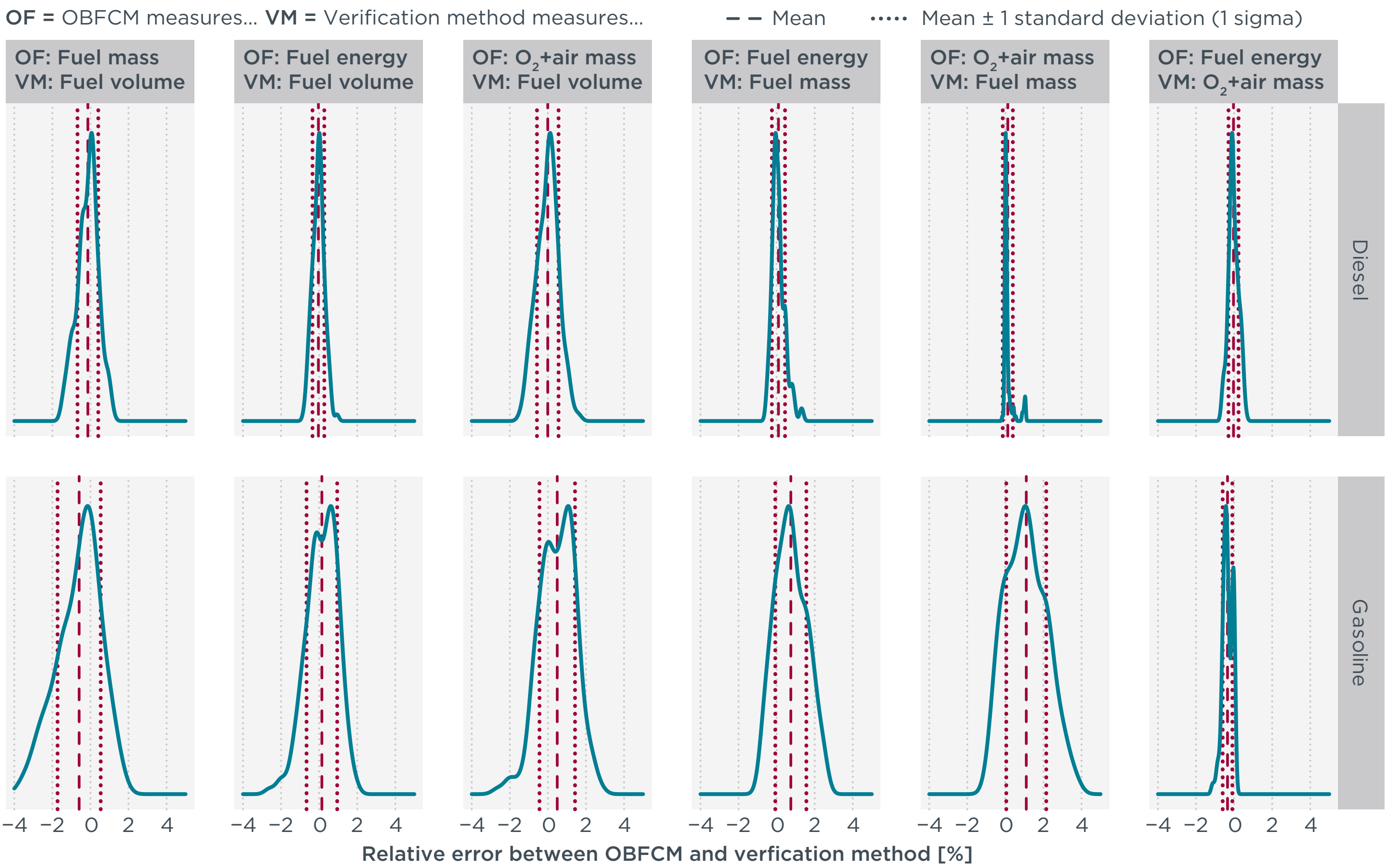

Figure 9. Error between OBFCM and verification method introduced by using market fuel instead of reference fuel. Each combination of potential OBFCM and verification measurement method is shown only once. When the methods applied by OBFCM and verification method are interchanged, the error distribution is mirrored at the zero-error line.

Table 14. Relative volumetric fuel consumption error introduced by using market fuel instead of reference fuel, dependent on OBFCM and verification method technology.

Verification method determines… → / OBFCM determines… ↓	Fuel type	Fuel volume	Fuel mass	O_2-concentration + air flow meter
Fuel volume	Gasoline	N/A	0.6 ±1.1	-0.5 ±0.9
	Diesel	N/A	0.1 ±0.5	0.0 ±0.6
Fuel mass	Gasoline	-0.6 ±1.1	N/A	-1.1 ±1.1
	Diesel	-0.1 ±0.5	N/A	-0.1 ±0.3
Fuel energy	Gasoline	0.1 ±0.8	0.7 ±0.8	-0.3 ±0.3
	Diesel	0.0 ±0.3	0.1 ±0.3	0.0 ±0.3
O_2-concentration + air flow meter	Gasoline	0.5 ±0.9	1.1 ±1.1	N/A
	Diesel	0.0 ±0.6	0.1 ±0.3	N/A

Notes: The values shown are the mean error and the 68% (1-sigma) confidence interval, both in %. The worst-case scenarios for diesel and gasoline are highlighted in red.

For gasoline, the errors show for most cases a wider confidence interval than for diesel as both gasoline E5 and E10 are available in the European Union while diesel is mainly B7. Having both E5 and E10 samples in the analysis also explains the humps visible in some of the gasoline-related curves. For diesel fuel, the mean error is in many cases at or close to zero. Based on the analysis, we arrive at an error margin for market fuel variability of ±2.2% in case of gasoline vehicles and ±0.6 % when testing diesel vehicles. If reference fuel is used, these uncertainties do not apply.

3.1.4. Combined OBFCM fuel consumption uncertainty during verification testing

Taking into account the uncertainties presented in the preceding sections, we calculated the total OBFCM accuracy that can reasonably be expected during type-approval or in-service conformity testing following the methodology presented in section 2.8.

Different uncertainties need to be considered, depending on whether OBFCM fuel consumption accuracy is verified on chassis dynamometer or during real-world testing and on the fuel used, as discussed in section 3.1. Table 15 summarizes the individual uncertainties stemming from the verification method, the OBFCM device itself, and the use of market fuel instead of reference fuel, and the combined uncertainty derived therefrom.

Table 15. Calculation of combined OBFCM fuel consumption accuracy when compared with reference method.

Uncertainty	Chassis dynamometer			Real-world driving		
	Reference fuel	Market fuel		Reference fuel	Market fuel	
Fuel type	Diesel & Gasoline	Diesel	Gasoline	Diesel & Gasoline	Diesel	Gasoline
Verification method vs. CVS	N/A	N/A		±2.5%	±2.5%	
OBFCM vs. verification method*	±1.55%	±1.55%		±2.1%	±2.1%	
Deviation from reference fuel	N/A	±0.6%	±2.2%	N/A	±0.6%	±2.2%
Combined (rounded)	±1.6%	±1.7%	±2.7%	±3.3%	±3.3 %	±3.9%

*CVS is verification method for chassis dynamometer tests

3.2. DRIVEN DISTANCE DETERMINATION

3.2.1. The accuracy of the real-world verification method

Test results

For real-world driving, GPS is used as verification for the OBFCM distance as described in section 2.6.2. To assess the accuracy of the GPS-based distance measurement, a reference distance signal is required. For this purpose, we compared the distance derived from GPS coordinates with the distance taken from an electronic map.

The relative distance error between the two methods is shown in Figure 10 for all valid RDE tests performed with the three test vehicles. Except for one test with the Audi, the results show high accuracy and precision. On average, the GPS underestimates the driven distance by 0.1% and the LoA_{95} range spreads by ±0.5% around this mean value. When considering the Audi measurement as an outlier, the LoA_{95} range shrinks even further to ±0.3%.

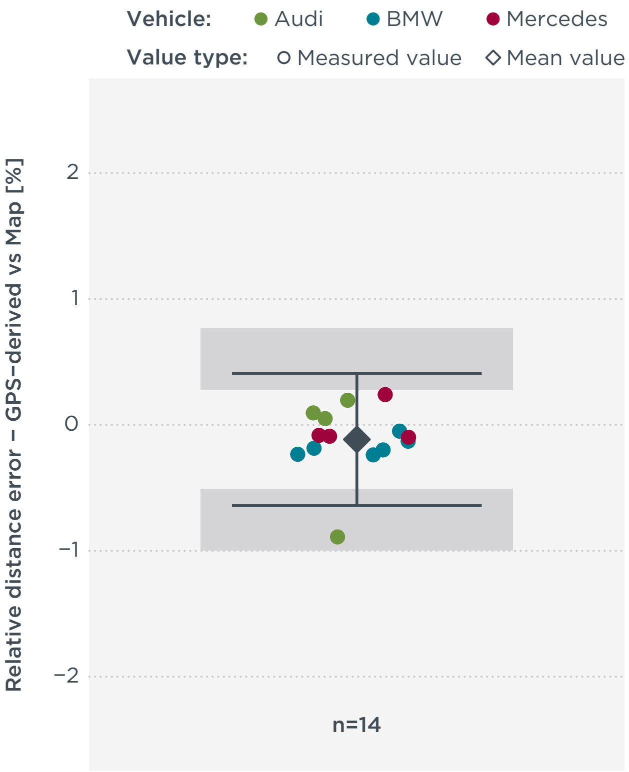

Figure 10. Relative error between GPS coordinates-based distance and distance derived from an electronic map. The error bars show the 95% level of agreement of the two methods and the grey rectangle reflects the 95% confidence interval of the upper and lower limit of the level of agreement.

Conclusion

Based on these results, we consider GPS to be a highly accurate method for verifying the OBFCM distance measurement. For developing reasonable real-world OBFCM distance accuracy requirements, we assume a verification method uncertainty of ±0.6%, which is the sum of absolute bias and LoA_{95} spread.

3.2.2. Accuracy of the test vehicles' OBFCM devices

We analyze the accuracy of the OBFCM distance measurement separately for tests performed on chassis dynamometer and real-world driving.

Test results for OBFCM accuracy on chassis dyno

For tests performed in the laboratory, the distance measured by the chassis dynamometer is used as the reference signal for determining the OBFCM accuracy. Figure 11 shows the mean error and the error per test between OBFCM and reference distance for tests performed in the laboratory. Excluded from the analysis are tests where the OBFCM distance signal acquisition is erroneous as well as the 3xNYCC test, due to its very short distance. The statistics are summarized in Table 16.

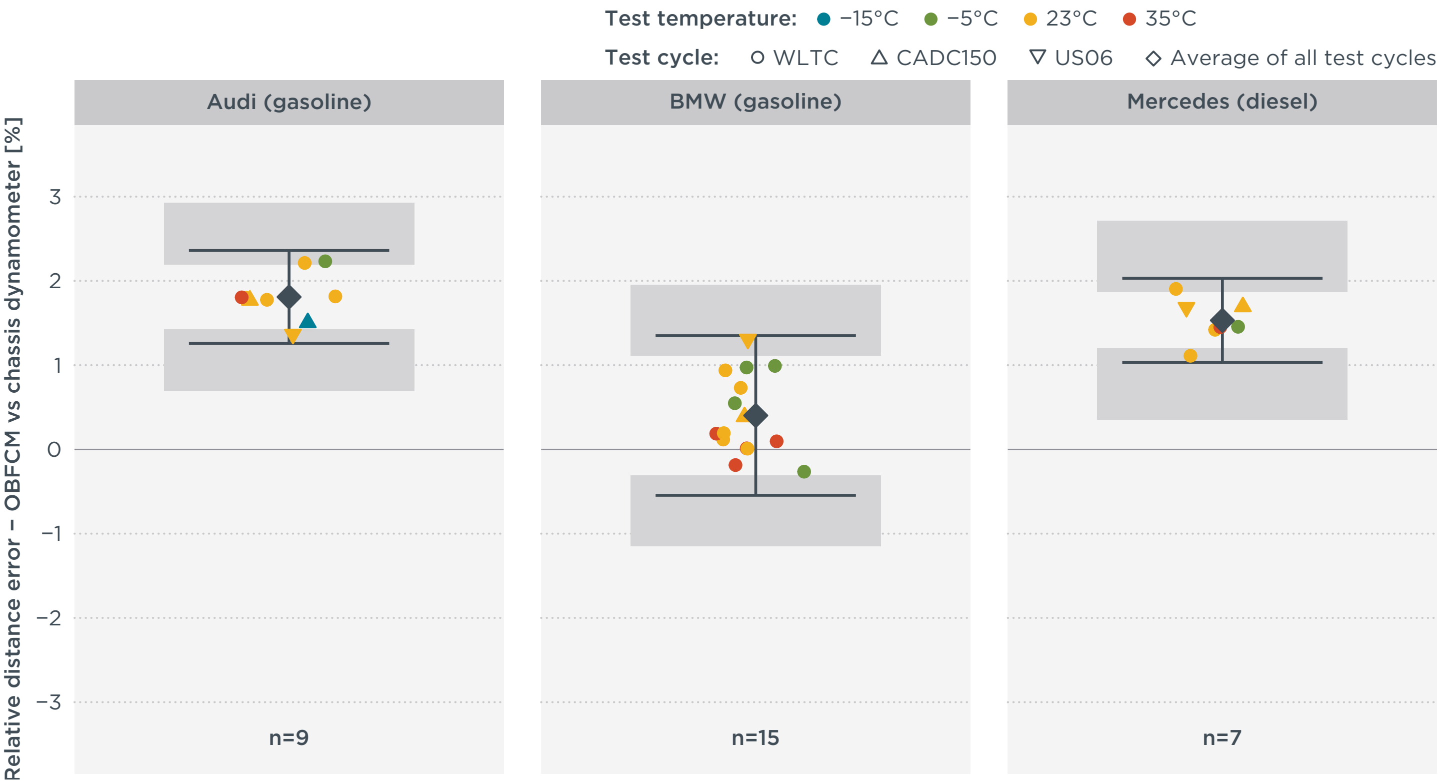

Figure 11. Relative error of OBFCM distance value when compared with the chassis dynamometer distance measurement. Due to the short distance, data from the 3xNYCC tests is not included in the analysis. The error bars show the 95% level of agreement between the two distance measurement methods and the grey rectangle reflects the 95% confidence interval of the upper and lower end of the level of agreement.

On all three vehicles, the OBFCM distance on average exceeds the chassis dynamometer value. The lowest bias of 0.4% is observed on the BMW, followed by 1.5% for the Mercedes, and 1.8% for the Audi. The spread of the LoA_{95} range around the mean is similar for the Audi and the Mercedes, with 0.6 and 0.5 of a percentage point, respectively. The BMW data shows a range of ±1.0 percentage point, almost twice as large. Figure 11 shows that the error is not systematically dependent on test type or ambient temperature.

Table 16. OBFCM distance error when compared with chassis dynamometer distance. The 3xNYCC tests are excluded.

Vehicle	No. of tests	Mean ±½ LoA_{95} range [%]	LoA_{95} 95% confidence interval	
			Inner [%]	Outer [%]
Audi	9	1.81 ±0.55	0.17	0.57
BMW	15	0.40 ±0.95	0.24	0.60
Mercedes	7	1.53 ±0.50	0.16	0.68

Test results for OBFCM accuracy during real-world driving

For assessing OBFCM accuracy under real-world conditions, the OBFCM distance measured during RDE and vehicle transfer tests was compared with the GPS coordinates-based distance, depicted in Figure 12 and summarized in Table 17.

Table 17. OBFCM distance measurement accuracy when compared with GPS coordinates-based distance during RDE and vehicle transfer tests.

Vehicle	Test type	No. of tests	Mean ±½ LoA_{95} range [%]	LoA_{95} 95% conf. interval	
				Inner [%]	Outer [%]
Audi	RDE & vehicle transfer tests	12	0.73 ±0.23	0.06	0.18
Audi	RDE test	4	0.80 ±0.22	0.09	0.70
Audi	Vehicle transfer tests	8	0.70 ±0.21	0.07	0.25
BMW	RDE & vehicle transfer tests	14	-0.29 ±0.39	0.10	0.26
BMW	RDE test	6	-0.31 ±0.15	0.05	0.25
BMW	Vehicle transfer tests	8	-0.28 ±0.52	0.16	0.60
Mercedes	RDE & vehicle transfer tests	8	-0.25 ±0.30	0.09	0.34
Mercedes	RDE test	4	-0.30 ±0.35	0.14	1.09
Mercedes	Vehicle transfer tests	4	-0.20 ±0.24	0.09	0.74

For all three vehicles, the OBFCM distance was in good agreement with the distance determined by the GPS verification method. The Mercedes and BMW OBFCMs slightly underestimate the driven distance on average by 0.3% for all real-world tests combined. For both vehicles, the OBFCM precision was also high as the narrow LoA_{95} ranges of ±0.3% for the Mercedes and ±0.4% for the BMW show.

The LoA_{95} range of the Audi of ±0.2% was even smaller than for the BMW and the Mercedes. However, the Audi was the only vehicle also overestimating the driven distance during real-world driving, on average by 0.7%. It should be noted that systematically overstating the driven distance by the OBFCM leads to an underestimation of the distance-specific fuel consumption.

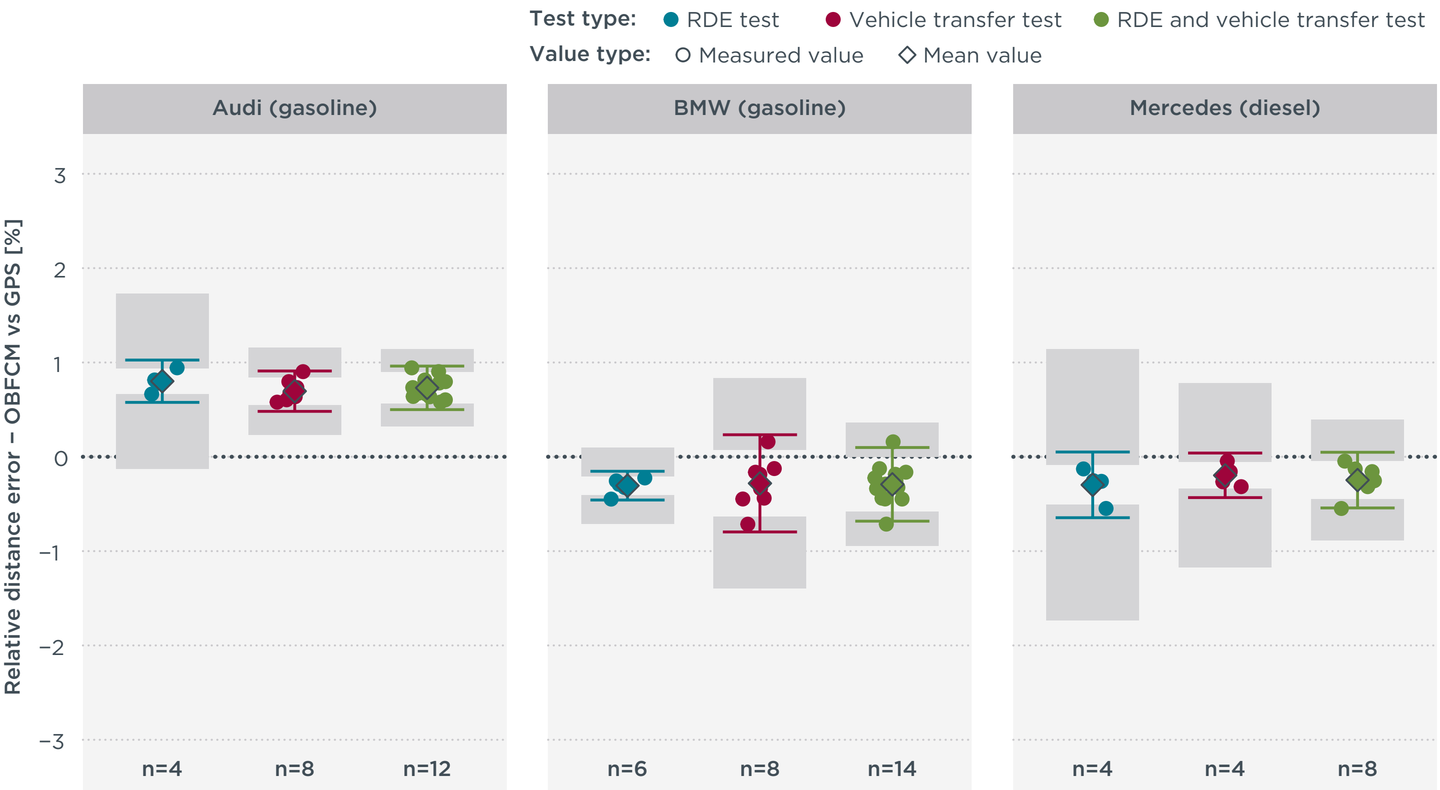

Figure 12. Relative error of OBFCM distance when compared with GPS coordinates-based distance for all RDE and vehicle transfer tests. The error bars show the 95% level of agreement between the two distance measurement methods and the grey rectangle reflects the 95% confidence interval of the upper and lower end of the level of agreement.

Conclusion

Our analysis shows that the OBFCM devices of all tested vehicles determine the driven distance with high precision and good accuracy, both on chassis dynamometer and during real-world driving. The data indicates that better OBFCM accuracy and precision is achieved on public roads than on chassis dynamometer. As explained in section 2.6.2, this might be due to differences in dynamic wheel radius used by the OBFCM for calculating vehicle speed. Higher wheel slip on chassis dynamometer could cause distance overestimation. However, as the OBFCM error observed on chassis dynamometer does not increase systematically for the more dynamic 3xUS06 tests, the tire slippage effect seems to be negligible. The higher accuracy during real-world driving could also indicate that the vehicle control systems use the on-board GPS for correcting the driven distance.

We expect that a systematic OBFCM distance error can be largely eliminated for chassis dynamometer tests under type-approval conditions. For this purpose, the tire dimension, model, age, and pressure used for calibrating the OBFCM should be made available by the manufacturer together with a correction factor for the OBFCM distance when tested on chassis dynamometer. This factor should account for the differences in tire pressure required for chassis dynamometer testing.

Under this assumption, the OBFCM accuracy requirement for chassis dynamometer testing can be based on the precision determined for the OBFCM devices. The similar OBFCM precision of both Audi and Mercedes show that even with current technology, a better precision than observed for the BMW on chassis dynamometer can be achieved. We therefore recommend an OBFCM device accuracy requirement of ±0.55% for chassis dynamometer testing under type-approval conditions when using the reference wheels declared by the manufacturer. Any systematic error due to vehicle-to-vehicle variability should be covered by this range as well, considering that currently no verifiable OBFCM distance accuracy requirements exist, so manufacturers were not obliged to put extra effort into achieving high distance accuracy.

Similarly, when performing real-world tests using the reference tires and settings used by the manufacturer in calibrating the OBFCM, no systematic error is expected. Based on the RDE and vehicle transfer test results, we consider a distance accuracy of ±0.35% for the OBFCM device under real-driving conditions as reasonable. That was the widest LoA_{95} range determined for all vehicles for the RDE tests. Again taking into account that the tested OBFCM devices were developed without any distance accuracy requirements, we expect this range to also cover any vehicle-to-vehicle variability of future OBFCM devices.

3.2.3. Other effects on OBFCM distance measurement accuracy

We assume that the OBFCM distance is based on the measured rotational wheel speed and calibrated dynamic wheel radius. However, the dynamic wheel radius is not constant but is affected by tire pressure, tire dimensions, and tread wear. This introduces uncertainties in the OBFCM distance measurement if not corrected.

Tire pressure

Based on literature research, a change in tire pressure below the regulatory detection threshold of 20% of the mandatory tire pressure monitoring systems can result in a maximum reduction of the dynamic circumference of about 0.4% (refer to section 2.7.2). The error to be considered can be halved to ±0.2% when the OBFCM control strategy always assumes as the current tire pressure the mean value of the last known pressure and the 20% lower detection threshold pressure.

Effect of tire dimension and tread wear

According to automobile associations, a tire with tread wear of 5 mm is considered as having reached its end of life. Applying this assumption, we calculated for each test vehicle the dynamic diameter of a new and an aged tire for all approved tire dimensions (refer to section 2.7.2). The relative deviation in dynamic diameter compared with the mean dynamic diameter of all tires considered are shown per vehicle in Figure 13. For minimal error, the OBFCM system can be calibrated for an average tire—a tire with a dynamic diameter of the arithmetic mean between a new tire with the largest dynamic radius and an end-of-life tire with the smallest radius. Under this assumption, the worst-case distance measurement error, observed on the Mercedes, would then be approximately ±1.6%.

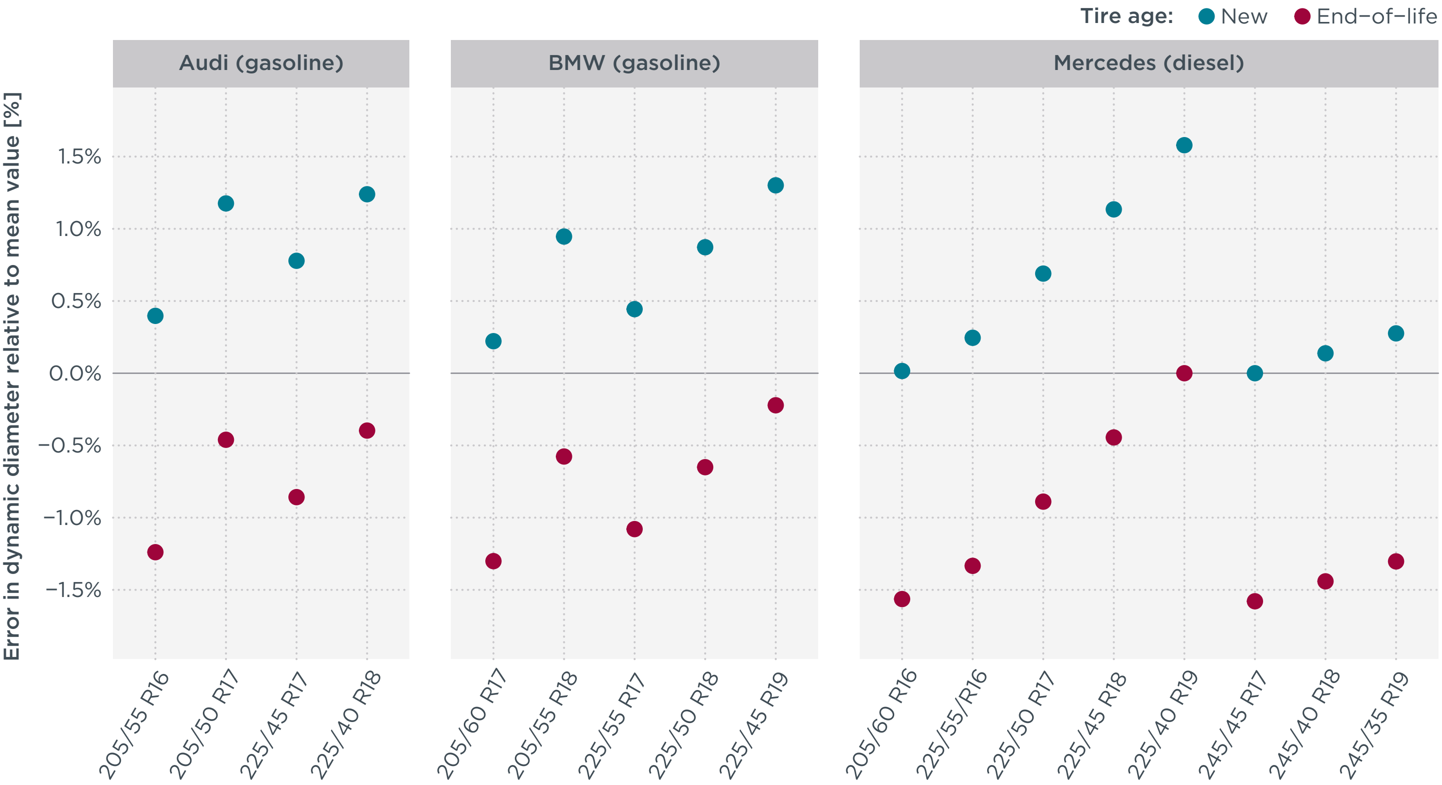

Figure 13. Variability of dynamic wheel diameter due to tire dimensions and ageing for all tire dimensions approved for each of the tested vehicles.

Total uncertainty

If not compensated for, the combined effect of tire pressure change, wheel dimension, and tread wear on the true dynamic wheel diameter could result in an OBFCM distance measurement error of approximately ±1.8%.

However, it is justified to expect that the dynamic wheel diameter value used by the OBFCM can be adapted during driving, considering the very high accuracy of the GPS-based distance measurement, as presented in section 3.2.1. As every vehicle is equipped with at least a GPS receiver in its eCall telemetry module,[8] this adaptation should be possible in any vehicle registered in the European Union without requiring additional hardware. Possibly, the accuracy of the eCall GPS receiver is lower than for the DGPS device used as verification method in this test project. However, more

8 eCall is the acronym for the pan-European in-vehicle emergency call system, which automatically transmits relevant data about vehicle, time, location, and driving direction to a 112-emergency call center in case of an accident. This technology is mandatory for new type approvals since March 31, 2018, for all passenger cars and light commercial vehicles.

detailed information about GPS signal quality and data about vehicle dynamics measured or calculated by the vehicle are available to the OBFCM for error correction. For real-world driving, where GPS data is available, we consider it therefore reasonable that the uncertainty stemming from tire pressure changes, wheel dimension variability, and tread wear can be at least halved to ±0.9%.

3.2.4. Combined OBFCM distance uncertainty during verification testing

Based on the individual uncertainties of verification method, OBFCM device, and use of random wheels instead of reference wheels, we calculated the combined OBFCM distance uncertainty to be considered when defining OBFCM accuracy requirements, shown in Table 18. Depending on whether the tests are performed on chassis dynamometer or on public roads and whether reference or random wheels are used, different uncertainties apply.

Table 18. Calculation of combined OBFCM distance accuracy when compared with reference method.

Uncertainty	Chassis dynamometer		Real-world driving	
	Reference wheels**	Random wheels	Reference wheels	Random wheels
GPS verification method vs electronic map	N/A	N/A	±0.6%	±0.6%
OBFCM vs verification method*	±0.55%	±0.55%	±0.35%	±0.35%
Deviation from standard tire	N/A	±1.8%	N/A	±0.9%
Combined (rounded)	**±0.6%**	**±1.9%**	**±0.7%**	**±1.1%**

* In laboratory, verification method is the signal from the chassis dynamometer. On road, the GPS coordinates-based distance is used.
** The same tire brand and model, dimensions, pressure, and tread wear as used for calibrating the OBFCM.

3.3. ELECTRIC ENERGY

The data recorded on the BMW X1 xDrive25e plug-in hybrid vehicle allowed also analyzing the PHEV-specific OBFCM parameters. The results of this analysis are presented in the following sections.

3.3.1. Accuracy of the HVBM verification method

Figure 14 shows for the six chassis dynamometer tests performed in charge-depleting mode the error between the accumulated current measured by the HVBM installed in the vehicle and the chassis dynamometer current clamp. The results show that both methods are in good agreement, with a mean error of -0.25% and an LoA_{95} spread of ±0.27 percentage points around the mean.

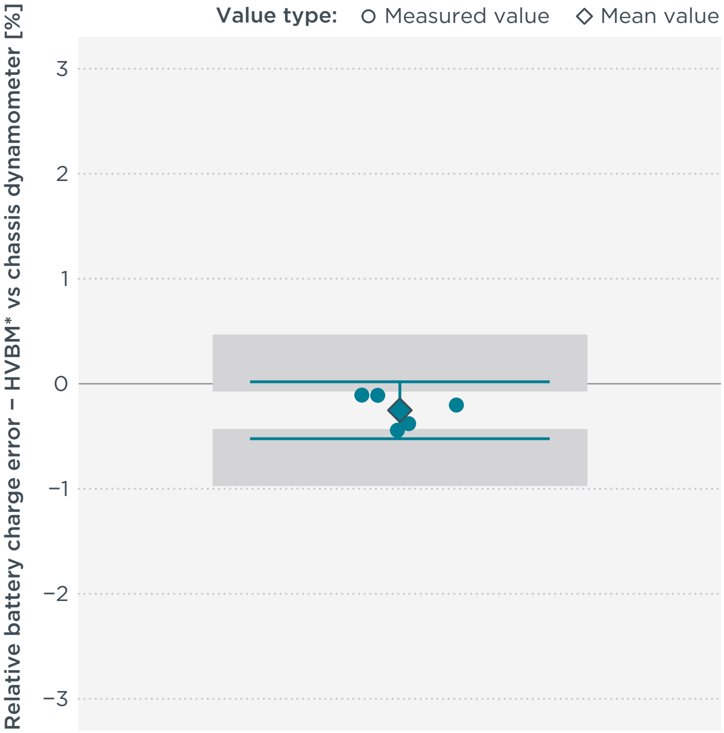

Figure 14. Relative error of battery charge measurement between the high-voltage breakout module (HVBM) installed in the vehicle and the chassis dynamometer bound current clamp. The measurements were performed on the BMW X1 plug-in hybrid vehicle during charge-depleting tests. *High-voltage breakout module for current and voltage measurement.

3.3.2. OBFCM accuracy of PHEV parameters

Test results for charged electric grid energy

The only electric energy parameter to be determined and stored compulsorily by the OBFCM is the total grid energy charged to the battery. Due to an error in the OBFCM implementation on the BMW, the recharged grid energy was recorded only during the vehicle transfer test phase (Dornoff, 2021). Therefore, data of only five battery recharge events were available for analyzing the accuracy of the OBFCM grid energy values. Due to the tight project timeline combined with a long duration for a full recharge because of low on-board charging power, only partial recharge events were recorded. This means that measurement data was available only for events where 1.5 kilowatt-hours to 4.2 kWh were recharged to the battery, while the usable traction battery capacity is 8.8 kWh, as presented in Figure 15.

The accuracy of the OBFCM grid energy value was determined by comparing the OBFCM recharged grid energy value and the recharged energy measured by the high-voltage breakout module during the recharge. Relative to the HVBM measurements, the OBFCM error for the recorded recharge events was between -0.5% and -4.7%. This error was much higher than expected. It was most likely due to the low resolution of the OBFCM grid energy value, which has a resolution of only one decimal place, as defined in the applicable OBD standards (SAE J1979-DA, 2019). For the low absolute values measured during recharge events, this can lead to very large rounding errors.

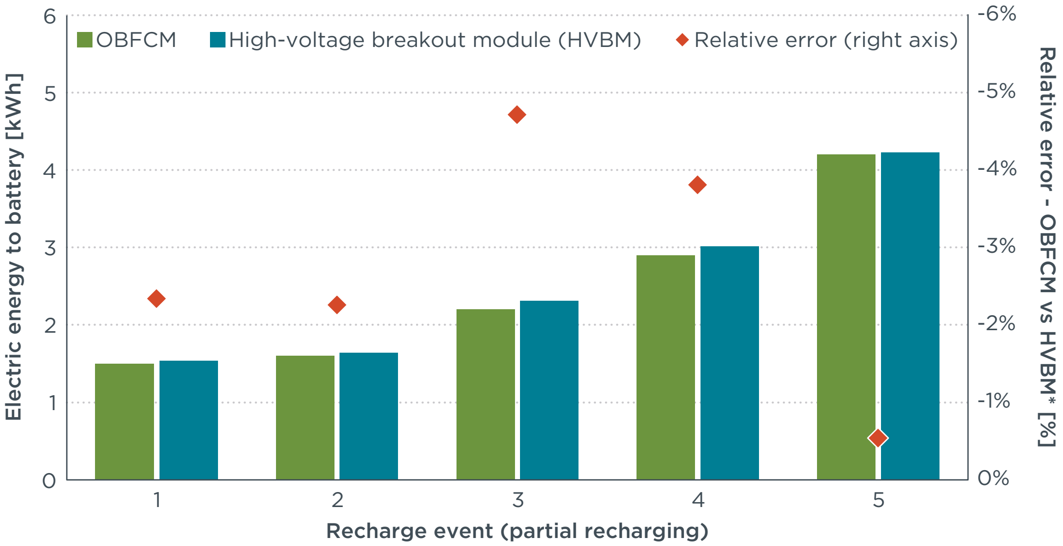

Figure 15. Total grid energy charged to battery, measured by OBFCM and high-voltage breakout module (HVBM) and the resulting error of the OBFCM relative to the HVBM measurement. *High-voltage breakout module for current and voltage measurement.

Test results for distance and fuel consumed in PHEV modes

While verifying OBFCM accuracy regarding driven distance and fuel consumption over an entire drive cycle can be considered straightforward, determining the OBFCM accuracy of PHEV operating mode-specific parameters cannot be accomplished in the same manner. This is because the present operating mode of a PHEV is usually not directly accessible to a third-party tester, as explained in section 2.6.4.

However, with the additional effort of polling the OBFCM lifetime values continuously and measuring the battery energy flow with the HVBM, it was possible to estimate the present operating mode and thereby to analyze whether the fuel consumption and distance values were assigned to the correct OBFCM operating mode counter. Since the overall accuracy of the OBFCM fuel consumption and distance measurement is investigated in sections 3.1.2 and 3.2.2, we focus here only on verifying whether the values in the PHEV modes match the total OBFCM values and whether they are assigned to the correct operating mode.

Figure 16 shows for two consecutive WLTCs in charge-depleting mode at -5°C the OBFCM distance (2nd graph from top) and fuel consumption (3rd graph from top) in the different PHEV operating modes together with the battery energy flow (left axis of bottom graph) and the battery and wheel power (right axis of bottom graph). The battery energy level or SoC shows that despite partial combustion engine operation, reflected in the engine speed signal in the top graph, the battery was on average depleted until about 3,420 seconds after test start. From there on, the SoC first slightly increases and then remains constant. While the battery is intermittently charged during the charge-depleting phase, indicated by a positive battery power, charging always occurs during deceleration phases when the wheel power is negative. However, after the switch from charge-depleting to charge-sustaining mode, the battery was also charged during periods of positive wheel power, when the power for charging the battery was generated by the combustion engine.

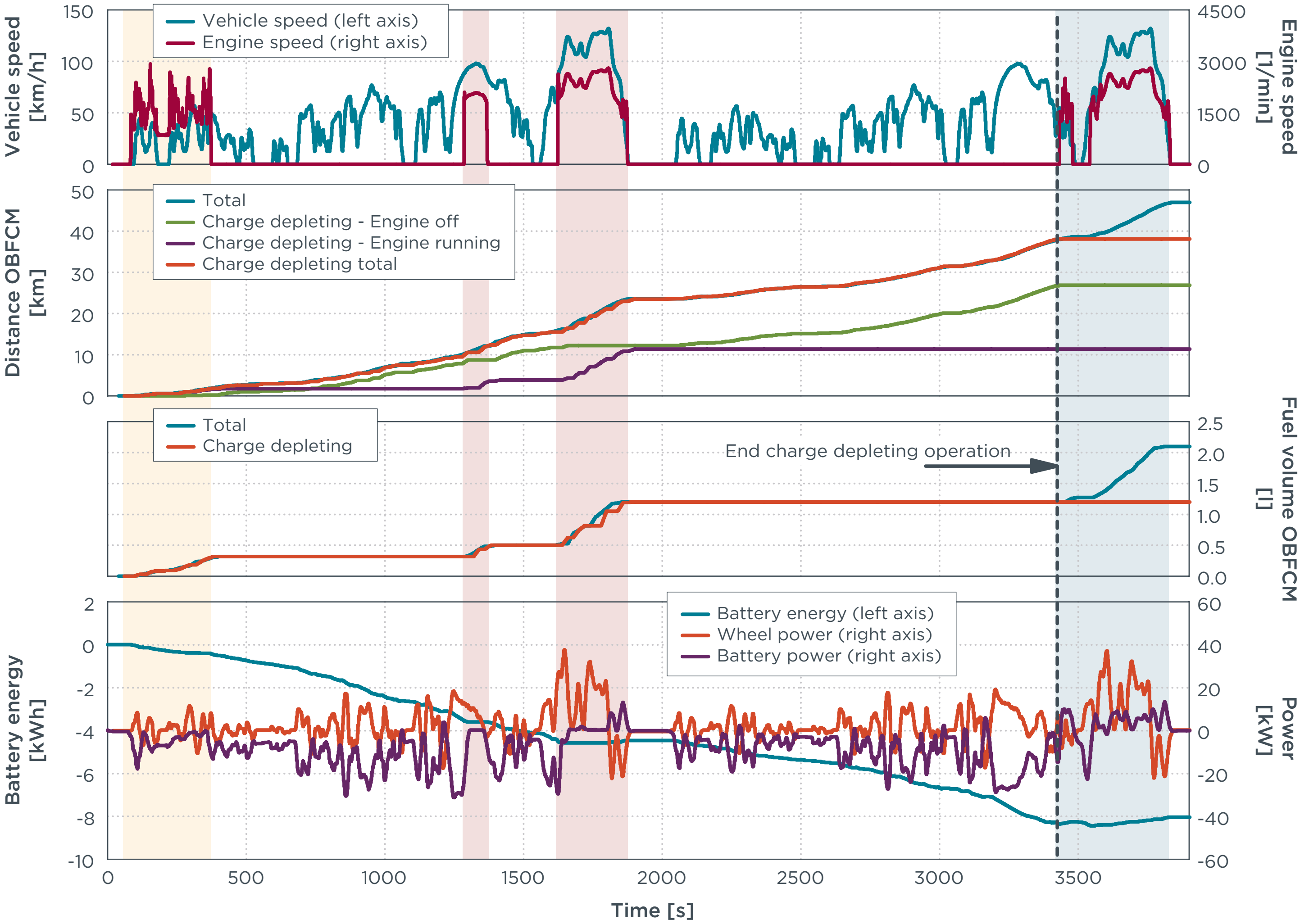

Figure 16. OBFCM plug-in hybrid vehicle specific distances and fuel consumption recorded for two consecutive WLTC tests in charge-depleting mode at -5°C. The yellow and red background indicates phases that are counted as "charge-depleting – engine running" mode by the OBFCM. However, the data shows that the vehicle operated in a charge-sustaining mode during the red-marked phases. The OBFCM considerred having reached charge-sustaining mode only when reaching the blue-marked phase.

The OBFCM signals for fuel consumption and distance in charge-depleting mode with the engine on and off reflected the observed behavior. When the engine was running (highlighted in Figure 16 by a yellow and red background), the counters for "charge-depleting – engine running" distance and fuel consumption increased. In phases where the vehicle was driven purely on electricity, or when the engine speed was zero and vehicle speed was greater than zero, the "charge-depleting engine-off" distance accumulated as expected, while the OBFCM fuel consumption value remained constant. At the end of the charge-depleting phase, the total OBFCM distance and fuel consumption in charge-depleting mode (red curves) matched the total OBFCM values (blue curves). Once the vehicle left charge-depleting mode, only the total OBFCM values kept increasing while the charge-depleting values froze, marked by a light blue background.

The OBFCM implementation on the vehicle followed the OBD definitions of charge-depleting and charge-sustaining operation, as the vehicle was considered to be in charge-sustaining mode when the target battery SoC was reached. However, the battery charge level was occasionally maintained at a constant level before reaching the target SoC (situations highlighted by a light red background in Figure 16). While the OBFCM counted these phases as being driven in charge-depleting mode, as the increasing "charge-depleting – engine running" OBFCM counters for distance and fuel consumption showed, we would consider these phases as being driven in charge-sustaining mode as no electric energy was consumed.

For verifying the correct distance and fuel consumption measurement by the OBFCM in user-selectable charge-increasing mode, data from a vehicle transfer test was used, shown in Figure 17. The periods where the battery energy measured by the HVBM increased continuously (highlighted in red) correlate well with the phases where the OBFCM charge-increasing distance signal rose (purple line in bottom graph). After a break, ending at 2,740 seconds elapsed cycle time, the vehicle was operated for approximately 650 seconds in charge-depleting mode until charge-increasing mode was engaged again. Both phases were correctly considered by the OBFCM as was the charge-increasing phase with a length of about 2,900 seconds starting at 5,160 seconds cycle time. When the HVBM-measured battery charge level reached 8.2 kWh, the vehicle switched to charge-sustaining mode, indicated by an almost constant battery charge level during the adjacent driving phase. At the same instant, the OBFCM charge-increasing mileage counter stopped.

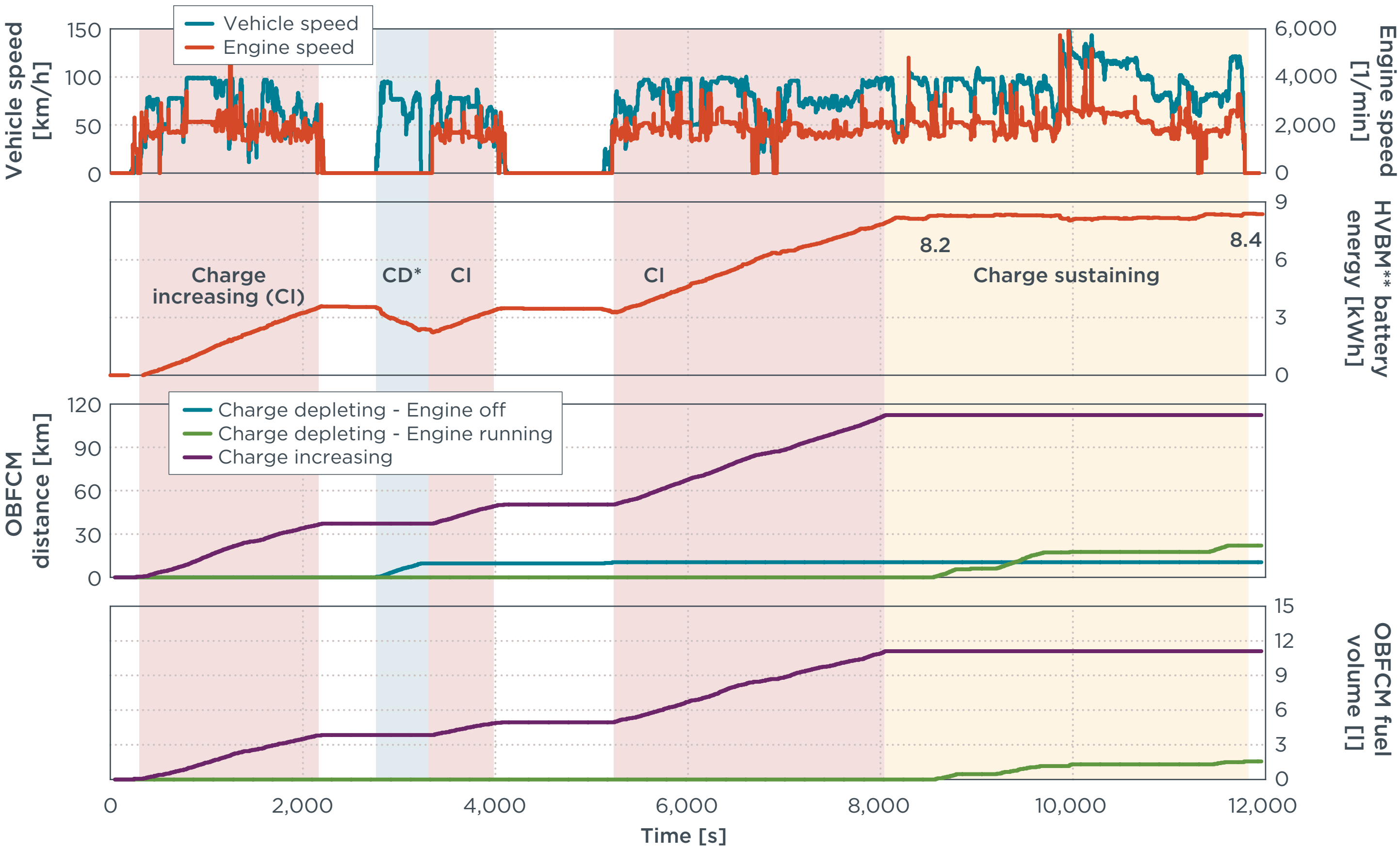

Figure 17. OBFCM distance and fuel consumption signals recorded during a vehicle transfer test in charge-depleting and charge-increasing operation.
*Charge depleting.
**High-voltage breakout module.

Conclusion

The analysis shows that distance and fuel consumption during the plug-in hybrid-specific operating modes were correctly assigned to the respective OBFCM values. However, this analysis could be performed only because we continuously polled the OBFCM lifetime values and installed an HVBM for monitoring the battery SoC. To allow for accuracy verification of these parameters during type-approval and in-service conformity testing, the vehicle needs to broadcast continuously at least the current operating mode and the instantaneous battery energy flow at the OBD interface. A safe and standardized access for measuring battery voltage and current on plug-in hybrid vehicles should be made mandatory.

4. SUMMARY AND RECOMMENDATIONS

This section summarizes the key findings of the analysis and presents recommendations for OBFCM fuel consumption and distance accuracy as well as plug-in hybrid vehicle-specific requirements. We also provide suggestions for improving the robustness of the OBFCM regulation.

OBFCM fuel consumption accuracy recommendations

For verifying the accuracy of OBFCM fuel consumption values, a reference method is required. On the chassis dynamometer, the CVS equipment used for type approval can be employed. For real-world driving, only portable measurement equipment can be used for verification. All investigated real-world verification methods showed good accuracy and are therefore considered as suited for verifying OBFCM fuel consumption. For deriving OBFCM fuel consumption accuracy requirements, the uncertainty of the verification method is factored in with ±2.5%, as shown in Table 19.

Table 19. OBFCM fuel consumption accuracy recommendations for chassis dynamometer and real-world verification testing.

Test environment:	Chassis dynamometer testing		Real-world testing	
Fuel type used:	Reference fuel	Market fuel	Reference fuel	Market fuel
Uncertainty of verification method Verification method ?= Reference method	N/A	N/A	±2.5%	±2.5%
Uncertainty of OBFCM* device OBFCM ?= Reference method**	±1.6%	±1.6%	±2.1%	±2.1%
Uncertainty from using market fuel	N/A	Diesel: ±0.6% Gasoline: ±2.2%	N/A	Diesel: ±0.6% Gasoline: ±2.2%
Combined accuracy recommendation:	**±1.6%**	**Diesel: ±1.7% Gasoline: ±2.7%**	**±3.3%**	**Diesel: ±3.3% Gasoline: ±3.9%**

* On-board fuel- and energy-consumption monitoring
** On chassis dynamometer, the CVS is used as reference. For real-world tests the verification methods, corrected for any systematic error when compared to CVS, are used as reference.

The accuracy of the OBFCM device at conditions similar to type approval and when using reference fuel is considered to be ±1.6%, based on tests performed on chassis dynamometer. Due to the wider range of dynamicity and operating conditions a vehicle encounters during real-world operation, the OBFCM device uncertainty for real-world testing is considered to be ±2.1%.

Using market fuel instead of reference fuel is expected to affect the OBFCM accuracy by ±0.6% for diesel and ±2.2% for gasoline.

Based on these individual uncertainties, we arrive at the recommendations for OBFCM fuel consumption accuracy presented in Table 19. ***When using reference fuel*** and the effect of market fuel variability does not need to be considered, we arrive at an accuracy requirement recommendation of ***±1.6% for chassis dynamometer testing and of ±3.3% when verified during real-world driving***. For tests performed with market fuel, it would be justified to ***require an accuracy on chassis dynamometer of ±1.7% for diesel and ±2.7% for gasoline, and for real-world tests of ±3.3% in the case of diesel and ±3.9% for gasoline.***

OBFCM distance accuracy recommendations

Similar to fuel consumption, we derived recommendations for OBFCM distance accuracy, based on the uncertainties applying during the chassis dynamometer and real-world tests. The results are summarized in Table 20.

Table 20. OBFCM distance accuracy recommendations for chassis dynamometer and real-world verification testing.

Test environment:	Chassis dynamometer testing		Real-world testing	
Wheels used:	Reference wheels	Random wheels	Reference wheels	Random wheels
Uncertainty of verification method Verification method ? = Reference method	N/A	N/A	±0.6%	±0.6%
Uncertainty of OBFCM* device OBFCM ? = Reference method**	±0.6%	±0.6%	±0.4%	±0.4%
Uncertainty from using random wheels	N/A	±1.8%	N/A	±0.9%
OBFCM accuracy recommendation:	**±0.6%**	**±1.9%**	**±0.7%**	**±1.1%**

* On-board fuel- and energy-consumption monitoring
** On chassis dynamometer, the distance determined by the chassis dynamometer is used as reference. For real-world tests, the verification method is used as reference.

The distance driven determined by the chassis dynamometer is used as reference value for OBFCM distance accuracy verification in the laboratory. For the real-world driving tests, we suggest using a GPS coordinates-based distance as the verification method. Based on our results, we consider this method to have an uncertainty of ±0.6%.

For the accuracy of the OBFCM device itself an uncertainty of ±0.6% seems justified for tests performed on chassis dynamometer when using reference wheels, or those with the same properties as used for OBFCM calibration. For real-world tests, our analysis suggests a slightly lower uncertainty of ±0.4%.

Using random wheels introduces an additional uncertainty of ±1.8% on chassis dynamometer. For real-world testing, we expect that the uncertainty can be partially mitigated using GPS data available in each vehicle, at least through the eCall telemetric module for correction, halving the uncertainty to ±0.9%.

Considering the uncertainties applicable for the different OBFCM accuracy verification test scenarios shown in Table 20, we can recommend an ***OBFCM distance accuracy requirement of ±0.6% on chassis dynamometer and ±0.7% for real-world driving, when using reference wheels. When random wheels are used, we recommend reducing the accuracy requirement to ±1.9% for chassis dynamometer testing and ±1.1% for tests on public roads.***

To support these OBFCM distance accuracy recommendations, manufacturers should declare which **tire dimension, model, age, and pressure was used for calibrating the OBFCM.** Furthermore, we recommend that manufacturers **provide a correction factor for the OBFCM distance when tested on chassis dynamometer** to account for the different tire pressure and tire-road contact geometry compared with real-world driving.

Plug-in hybrid vehicle OBFCM parameters

Our analysis revealed some challenges for verifying the PHEV-specific OBFCM parameters. Based on our findings, we offer the following recommendations:

We recommend defining accuracy requirements for recharged grid energy. However, for verifying the accuracy of this parameter for single recharge events conducted on chassis dynamometer or during real-world operation, ***the OBFCM recharged grid energy value needs to be reported with higher resolution*** than the one decimal currently defined in the OBD standards. We also noted that the OBFCM grid energy value does not include on-board charger losses. To allow for a comparison of the OBFCM value with the energy supplied by external chargers to the vehicle, ***we recommend that on-board charger efficiency be determined during type approval and made available in the certificate of conformity or transparency list.***

Further, ***we recommend introducing accuracy requirements for OBFCM distance and fuel consumption in charge-depleting and charge-increasing modes.*** The accuracy limits should be the same as for total OBFCM distance and fuel consumption. To allow for accuracy verification of these parameters during approval and in-service conformity testing, ***the vehicle needs to broadcast continuously at least the current operating mode and the instantaneous battery energy flow*** at the OBD interface. Furthermore, a ***safe and standardized access for measuring battery voltage and current*** on all plug-in hybrid vehicles is needed.

Other recommendations

Based on observations made during the test project and the subsequent data analysis, we also recommend:

It should be mandatory that accumulated second-by-second OBFCM values equal the lifetime values. On all vehicles, we observed a discrepancy between lifetime distance and fuel volume and the accumulated OBFCM vehicle speed and volumetric fuel flow signal. As both lifetime and integrated second-by-second values report the same physical parameters, they should be identical.

The OBFCM values should not have a systematic offset. Manufacturers might attempt to artificially reduce the real-world to type-approval gap by exploiting the OBFCM distance and fuel consumption accuracy requirements. To prevent this, it should be required that the OBFCM data has no systematic offset.

The volumetric OBFCM fuel consumption should relate to density at 15°C. Neither type-approval regulation (EU) 2017/1151 nor OBD standards SAE J1979 defines reference conditions for the volumetric OBFCM fuel consumption. For comparability with type-approval values, OBFCM fuel consumption needs to be reported for the same reference temperature.

To ensure that OBFCM data are suitable for monitoring the gap between real-world CO_2 emissions and type-approval values, accurate OBFCM data is required. The presented analysis shows that the accuracy of current OBFCM devices justifies tight accuracy requirements for both chassis dynamometer and on-road testing and that suitable methods for verifying OBFCM fuel consumption and distance values should be available.

REFERENCES

ADAC. (2021, February 4). *Mindestprofiltiefe bei Winter- und Sommerreifen [Miminum tread depth of winter and summer tires] | ADAC*. https://www.adac.de/rund-ums-fahrzeug/ausstattung-technik-zubehoer/reifen/sicherheit/reifenprofil/

Anghelache, G., & Moisescu, R. (2017). The measurement of dynamic radii for passenger car tyre. *IOP Conference Series: Materials Science and Engineering*, *252*, 012014. https://doi.org/10.1088/1757-899X/252/1/012014

AvD e.V. (2021a, August 4). *Kampagne „Profil schon gecheckt?" [Campaign "Tread depth checked?"]*. Automobilclub von Deutschland e.V. https://www.avd.de/mein-club/avd-der-club/presse/kampagnen/profil-schon-gecheckt

AvD e.V. (2021b, August 26). *Winterreifenpflicht [Obligation to use winter tires]*. Automobilclub von Deutschland e.V. https://www.avd.de/wissen/recht/verkehrsvorschriften-ausland/winterreifenpflicht

Bland, J. M., & Altman, D. G. (1999). *Measuring agreement in method comparison studies*. *8*(2), 135–160. https://doi.org/10.1177/096228029900800204

Bonfig, K.-W., Drahm, W., Mágori, V., Höcker, R., Konzelmann, U., & Rieder, A. (2014). Sensorik zur Durchflussmessung [Flow metering sensors]. In H.-R. Tränkler & L. Reindl (Eds.), *Sensortechnik* (pp. 793–901). Springer Berlin Heidelberg. https://doi.org/10.1007/978-3-642-29942-1_13

Bosch. (2021, March 4). *Wideband lambda sensor*. https://www.bosch-mobility-solutions.com/en/products-and-services/commercial-vehicles/powertrain-systems/natural-gas/wideband-lambda-sensor/

Carkeet, A. (2015). Exact parametric confidence intervals for Bland-Altman limits of agreement. *Optometry and Vision Science*, *92*(3), e71–e80. https://doi.org/10/f64dqs

Continental. (2020). *Tyre Databook 2020—2021 Car—4x4—Van*. Continental Reifen Deutschland GmbH. http://blobs.continental-tires.com/www8/servlet/blob/85806/69977261017e17f2a1dc8054655a4bcf/download-technical-databook-data.pdf

CSM GmbH. (2021). *CSM HV breakout module typ 1.1/1.2*. https://www.csm.de/en/products/hv-breakout-modules/hv-breakout-modules-1-x#data

Dornoff, J. (2021). *Plug-in hybrid vehicle CO_2 emissions: How they are affected by ambient conditions and driver mode selection* (p. 57) [White Paper]. ICCT. https://theicct.org/publications/phev-co2-emissions-ambient-conditions-dec2021

Dornoff, J., & Rodríguez, F. (2019). *Gasoline versus diesel: Comparing CO_2 emission levels of a modern medium size car model under laboratory and on-road testing conditions*. International Council on Clean Transportation. https://theicct.org/publications/gasoline-vs-diesel-comparing-co2-emission-levels

EEA. (2021). *ETC/CME Report 1/2021: Fuel quality monitoring in the EU in 2019.* (Eionet report-ETC/CME 1/2021). European Environment Agency. https://www.eionet.europa.eu/etcs/etc-cme/products/etc-cme-report-1-2021-fuel-quality-monitoring-in-the-eu-in-2019

Commission Regulation (EU) 2017/1151 of 1 June 2017 supplementing Regulation (EC) No. 715/2007 of the European Parliament and of the Council on type-approval of motor vehicles with respect to emissions from light passenger and commercial vehicles (Euro 5 and Euro 6) and on access to vehicle repair and maintenance information, amending Directive 2007/46/EC of the European Parliament and of the Council, Commission Regulation (EC) No 692/2008 and Commission Regulation (EU) No. 1230/2012 and repealing Commission Regulation (EC) No 692/2008, Pub. L. No. OJ L 157,01.06.2017, 1 (2017). http://data.europa.eu/eli/reg/2017/1151/oj

Regulation (EC) No. 661/2009 of the European Parliament and of the Council of 13 July 2009 concerning type-approval requirements for the general safety of motor vehicles, their trailers and systems, components and separate technical units intended therefor, Pub. L. No. (EC) No. 661/2009, 32009R0661 (2009). http://data.europa.eu/eli/reg/2009/661/2019-04-24

Regulation (EU) 2019/631 of the European Parliament and of the Council of 17 April 2019 setting CO_2 emission performance standards for new passenger cars and for new light commercial vehicles and repealing regulations (EC) No. 443/2009 and (EU) No. 510/2011 (Text with EEA relevance.), Pub. L. No. 32019R0631, 111 OJ L 13 (2019). http://data.europa.eu/eli/reg/2019/631/oj/eng

Fantner, G. (2013). *A brief introduction to error analysis and propagation*. EPFL. https://www.epfl.ch/labs/lben/wp-content/uploads/2018/07/Error-Propagation_2013.pdf

Geng, P., Furey, R., & Konzack, A. (2010). Calculation of heating value for gasoline containing ethanol. *SAE International Journal of Fuels and Lubricants*, *3*(2), 229–237. https://doi.org/10.4271/2010-01-1517

Grouven, U., Bender, R., Ziegler, A., & Lange, S. (2007). Vergleich von Messmethoden [Comparison of measurement methods]. *DMW - Deutsche Medizinische Wochenschrift*, *132*(S 01), e69–e73. https://doi.org/10/bdz6xh

ISO. (2015, August). *ISO 15031-5:2015(en), Road vehicles—Communication between vehicle and external equipment for emissions-related diagnostics—Part 5: Emissions-related diagnostic services*. https://www.iso.org/obp/ui/#iso:std:iso:15031:-5:ed-3:v1:en

Lopes, S. M., Furey, R., & Geng, P. (2013). Calculation of heating value for diesel fuels containing biodiesel. *SAE International Journal of Fuels and Lubricants*, *6*(2), 407–418. https://doi.org/10.4271/2013-01-1139

MECA. (2020). *A statutory and regulatory history of the U.S. evaporative requirements for motor vehicles and analysis of European evaporative emission requirements*. Manufacturers of Emission Controls Association. http://www.meca.org/resources/US_Evap_History_and_General_Findings_1-31-20_FINAL.pdf

J1979-DA, Digital annex of E/E diagnostic test modes, J1979DA_201905 J1979DA (2019). https://www.sae.org/standards/content/j1979da_201905/

Silvis, W. M. (1997). An algorithm for calculating the air/fuel ratio from exhaust emissions. *Engine Modeling (SP-1255)*, *970514*. https://doi.org/10.4271/970514

Tietge, U., Díaz, S., Mock, P., Bandivadekar, A., Dornoff, J., & Ligterink, N. (2019). *From laboratory to road: A 2018 update*. International Council on Clean Transportation. https://theicct.org/publications/laboratory-road-2018-update

Regulation 141—Addendum 140 uniform provisions concerning the approval of vehicles with regard to their tyre pressure monitoring systems (TPMS), Pub. L. No. UN/ECE R 141, ECE/TRANS/WP.29/2016/63. (2017). https://unece.org/fileadmin/DAM/trans/main/wp29/wp29regs/2017/R141e.pdf

Wolf, H. (2015). *Transport properties of fuels* (p. 4244355 bytes) [PDF]. Physikalisch-Technische Bundesanstalt (PTB). https://doi.org/10.7795/110.20150622W

APPENDICES

APPENDIX 1: RDE TEST ROUTES

Figure A1 shows the vehicle speed and elevation profile recorded during two RDE tests on route 1 and 2.

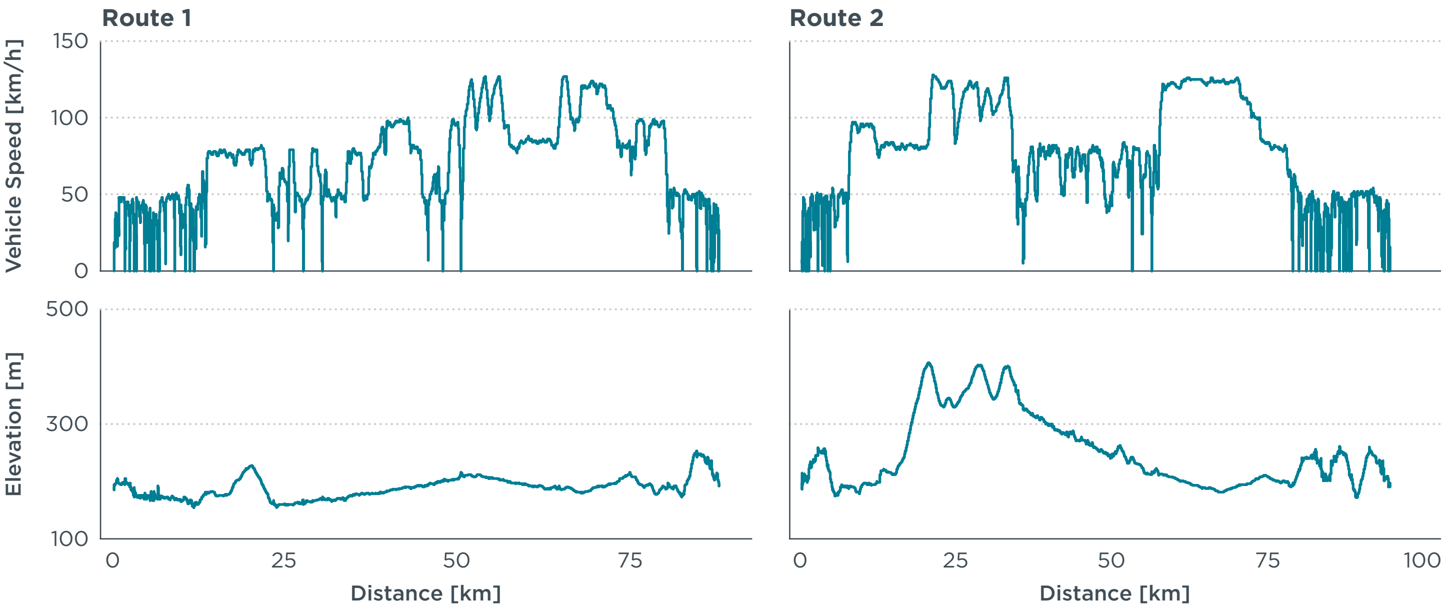

Figure A1. Sample vehicle speed trace and elevation profile of RDE test routes 1 and 2

APPENDIX 2: UNCERTAINTY CALCULATION FOR MARKET FUEL

The error introduced by using market fuel instead of reference fuel depends on the underlying measurement principle of both OBFCM and verification method. For isolating the fuel composition effect, we made the following assumptions for the error analysis:

- The values measured by the OBFCM and verification method are accurate. For example, if the OBFCM measures volumetric fuel flow, we assume that the measured fuel flow coincides with the real volumetric fuel flow to the engine.
- Both OBFCM and verification method are calibrated for reference fuel. This means, for example, that in the case of the (O_2+AFM) carbon balance method, the air-fuel ratio is calculated from the oxygen concentration using the hydrogen-to-carbon and oxygen-to-carbon ratio of the reference fuel.
- The relative error in all cases is calculated as one minus the ratio of volumetric fuel consumption of OBFCM and the verification method, regardless of the underlying measurement principle. This means that the measured values are always converted to a fuel volume.

Under these assumptions, we derived the following equations to calculate the fuel volume ratios.

OBFCM measures fuel volume – Verification method measures fuel volume. In this case both systems measure the same parameter, and therefore no error is introduced when using market fuel instead of reference fuel. However, both methods need to provide the volumetric fuel consumption for the same reference fuel temperature.

OBFCM measures fuel mass – Verification method measures fuel volume. To provide a fuel volume signal v_{OBFCM}, the measured OBFCM fuel mass m_{OBFCM} is converted to a volume using the calibrated density ρ_{ref} of the reference fuel at 15°C. The true fuel volume measured by the verification method $v_{verification}$ is equivalent to the true fuel mass m_{real} when using the actual density ρ_{real} of the fuel at 15°C. Considering the assumption that the OBFCM measures the true fuel mass, that is $m_{OBFCM} = m_{real}$, the fuel volume ratio calculates as follows:

$$ratio_{mass/vol} = \frac{v_{OBFCM}}{v_{verification}} = \frac{\frac{m_{OBFCM}}{\rho_{ref}}}{\frac{m_{real}}{\rho_{real}}} = \frac{\rho_{real}}{\rho_{ref}}$$

OBFCM measures fuel energy – Verification method measures fuel volume. To provide a fuel volume signal v_{OBFCM}, the OBFCM fuel energy egy_{OBFCM} measurement is converted by applying the calibrated lower heating value of the reference fuel LHV_{ref} and the density ρ_{ref} of the reference fuel at 15°C. The fuel volume measured by the verification method $v_{verification}$ is equivalent to the true fuel energy egy_{real} when using the actual lower heating value LHV_{real} and density ρ_{real} at 15°C of the fuel used. Considering the assumption that the OBFCM measures the true fuel energy, that is $egy_{OBFCM} = egy_{real}$, the fuel volume ratio calculates as follows:

$$ratio_{energy/vol} = \frac{v_{OBFCM}}{v_{verification}} = \frac{\frac{egy_{OBFCM}}{LHV_{ref} \times \rho_{ref}}}{\frac{egy_{real}}{LHV_{real} \times \rho_{real}}} = \frac{LHV_{real} \times \rho_{real}}{LHV_{ref} \times \rho_{ref}}$$

OBFCM measures O_2 concentration and air mass flow – Verification method measures fuel volume. To derive the OBFCM fuel volume, first the O_2 concentration $c_{O2,OBFCM}$ needs to be converted to the air-fuel equivalence ratio λ_{OBFCM}, using the molar hydrogen/carbon ratio $r_{HC,ref}$ and oxygen/carbon ratio $r_{OC,ref}$ of the reference fuel:

$$\lambda_{OBFCM,ref} = \frac{1 + \frac{c_{O2,OBFCM}}{1 + \frac{4}{r_{HC,ref}} - 2 \times \frac{r_{OC,ref}}{r_{HC,ref}}}}{1 - 4.762 \times c_{O2,OBFCM}}$$

Together with the air mass flow $m_{Air,OBFCM}$, and both the stoichiometric air-fuel-ratio $AFR_{St,ref}$ and density ρ_{ref}, of the reference fuel, the equivalent OBFCM fuel volume can be calculated as follows:

$$v_{OBFCM} = m_{Fuel,OBFCM} \times \frac{1}{\rho_{ref}} = \frac{m_{Air,OBFCM}}{AFR_{St,ref} \times \lambda_{OBFCM,ref}} \times \frac{1}{\rho_{ref}}$$

The fuel volume measured by the verification method $v_{verification}$ can be converted to the true oxygen concentration and true air mass by calculating the true air-fuel equivalence ratio λ_{real} and stoichiometric air-fuel ratio $AFR_{St,ref}$ using the H/C and O/C ratios of the fuel in use. The error from deviations between market fuel and reference fuel then results in:

$$ratio_{O2+AFM/vol} = \frac{v_{OBFCM}}{v_{verification}} = \frac{\frac{m_{air,OBFCM}}{\lambda_{OBFCM,ref} \times AFR_{St,ref}} \times \frac{1}{\rho_{ref}}}{\frac{m_{air,real}}{\lambda_{real} \times AFR_{St,real}} \times \frac{1}{\rho_{real}}} = \frac{\rho_{real} \times \lambda_{real} \times AFR_{St,real}}{\rho_{ref} \times \lambda_{OBFCM,ref} \times AFR_{St,ref}}$$

OBFCM measures fuel volume – Verification method measures fuel mass. In this case, the fuel volume measured by the OBFCM is equivalent to the real fuel mass by dividing it by the true density ρ_{real} at 15°C. According to the assumptions, the verification method converts the measured fuel mass $m_{verification}$ to a fuel volume using the reference fuel density ρ_{ref}. The ratio of OBFCM and verification method fuel volume therefore calculates as follows:

$$ratio_{vol/mass} = \frac{v_{OBFCM}}{v_{verification}} = \frac{m_{OBFCM} \times \frac{1}{\rho_{real}}}{m_{verification} \times \frac{1}{\rho_{ref}}} = \frac{\rho_{ref}}{\rho_{real}}$$

OBFCM measures fuel mass – Verification method measures fuel mass. Both methods measure the real fuel mass and apply the reference density ρ_{ref} to determine the fuel volume. Therefore, no error is introduced in this case.

OBFCM measures fuel energy – Verification method measures fuel mass. To provide a volumetric fuel consumption value, the fuel energy measured by the OBFCM egy_{OBFCM} is converted using the density and lower heating value of the reference fuel.

$$v_{OBFCM} = \frac{egy_{OBFCM}}{LHV_{ref}} \times \frac{1}{\rho_{ref}}$$

The fuel mass measured by the verification method $m_{verification}$, is converted to a fuel volume using the reference fuel density ρ_{ref} as well. Since $m_{verification}$ is the true fuel mass, it is equivalent to the ratio of real fuel energy and the lower heating value of the fuel used. Considering that the OBFCM measures the real fuel energy, the following formula for calculating the ratio of OBFCM and verification method fuel volume is derived:

$$ratio_{energy/vol} = \frac{v_{OBFCM}}{v_{verification}} = \frac{\frac{egy_{real}}{LHV_{ref}} \times \frac{1}{\rho_{ref}}}{\frac{egy_{real}}{LHV_{real}} \times \frac{1}{\rho_{ref}}} = \frac{LHV_{real}}{LHV_{ref}}$$

OBFCM measures exhaust O_2 concentration and air mass flow – Verification method measures fuel mass. In this case, the OBFCM measures the true O_2 concentration and air mass flow, which is converted to a fuel volume using the calibrated reference fuel properties:

$$v_{OBFCM} = \frac{m_{air,OBFCM}}{\lambda_{OBFCM,ref} \times AFR_{St,ref}} \times \frac{1}{\rho_{ref}}$$

The true fuel mass determined by the verification method $m_{verification}$ is equivalent to the ratio of true air mass $m_{air,real}$ and the product of true air-fuel equivalence ratio λ_{real} and stoichiometric air-fuel ratio $AFR_{St,real}$ of the fuel used. Conversion to fuel volume $v_{verification}$ is established using the reference density ρ_{ref} Considering that the air mass measured by the OBFCM is the true air mass $m_{air,real}$ results in the following equation:

$$ratio_{CO_2/vol} = \frac{v_{OBFCM}}{v_{verification}} = \frac{\frac{m_{air,OBFCM}}{\lambda_{OBFCM,ref} \times AFR_{St,ref}} \times \frac{1}{\rho_{ref}}}{\frac{m_{air,real}}{\lambda_{real} \times AFR_{St,real}} \times \frac{1}{\rho_{ref}}} = \frac{\lambda_{real} \times AFR_{St,real}}{\lambda_{OBFCM,ref} \times AFR_{St,ref}}$$

OBFCM measures fuel energy – Verification method determines oxygen concentration and air mass flow. In this case, the fuel volume needs to be calculated by both OBFCM and verification method. The OBFCM fuel volume, based on the measured energy is calculated using the reference fuel properties as:

$$v_{OBFCM} = m_{OBFCM} \times \frac{1}{\rho_{ref}} = \frac{egy_{OBFCM}}{LHV_{ref}} \times \frac{1}{\rho_{ref}}$$

The fuel volume of the verification method $v_{verification}$ can be derived from the measured O_2-concentration and air mass flow using the reference fuel properties by the following equation:

$$v_{verification} = m_{verification} \times \frac{1}{\rho_{ref}} = \frac{m_{air,real}}{\lambda_{ref} \times AFR_{st,ref}} \times \frac{1}{\rho_{ref}}$$

The true air mass $m_{air,real}$ depends on the true fuel energy egy_{real} as defined as follows:

$$m_{air,real} = m_{fuel,real} \times AFR_{St,real} \times \lambda_{real} = \frac{egy_{fuel,real}}{LHV_{real}} \times AFR_{St,real} \times \lambda_{real}$$

Considering that the OBFCM measures the true fuel energy egy_{real}, the ratio of OBFCM and verification method fuel volume, is calculated as follows:

$$ratio_{energy/CO_2} = \frac{v_{OBFCM}}{v_{verification}} = \frac{LHV_{real}}{LHV_{ref}} \times \frac{\lambda_{ref} \times AFR_{St,ref}}{\lambda_{real} \times AFR_{St,real}}$$

The equations presented in this section are summarized in Table A1. It shows that in cases where the measurement methods of OBFCM and verification method are switched, the ratio of OBFCM and verification method fuel volume is reciprocal.

Table A1. Formulas for calculating the effect of using market fuel instead of reference fuel on the ratio of volumetric OBFCM and verification method fuel consumption. VM: Verification method

VM → OBFCM ↓	Fuel volume	Fuel mass	O_2 + AFM
Fuel volume	No error	$\frac{\rho_{ref}}{\rho_{real}}$	$\frac{\rho_{ref} \times \lambda_{ref} \times AFR_{St,ref}}{\rho_{real} \times \lambda_{real} \times AFR_{St,real}}$
Fuel mass	$\frac{\rho_{real}}{\rho_{ref}}$	No error	$\frac{\lambda_{ref} \times AFR_{St,ref}}{\lambda_{real} \times AFR_{St,real}}$
Fuel energy	$\frac{LHV_{real} \times \rho_{real}}{LHV_{ref} \times \rho_{ref}}$	$\frac{LHV_{real}}{LHV_{ref}}$	$\frac{LHV_{real} \times \lambda_{ref} \times AFR_{St,ref}}{LHV_{ref} \times \lambda_{real} \times AFR_{St,real}}$
O_2+AFM	$\frac{\rho_{real} \times \lambda_{real} \times AFR_{St,real}}{\rho_{ref} \times \lambda_{ref} \times AFR_{St,ref}}$	$\frac{\lambda_{real} \times AFR_{St,real}}{\lambda_{ref} \times AFR_{St,ref}}$	No error

Note: With ρ_i as fuel density, LHV_i as fuel lower heating value, $\lambda_{Exh,i}$ as the air-fuel equivalence ratio and $AFR_{St,i}$ as the stoichiometric air-fuel ratio. For index i, "*ref*" is used for reference fuel properties and "*real*" is used for the properties of the real fuel used, that is market fuel.

Calculation of lower heating value

The lower heating value (LHV) of gasoline fuel, required for the analysis, was calculated using an equation developed by SGS and BMW for fuels with less than 10% ethanol content, presented for example in Geng et al. (2010). The equation for gasoline is based on a regression analysis using carbon, hydrogen, and oxygen content as the independent variables:

$$LHV_{gasoline}\left[\frac{MJ}{kg}\right] = 0.022 + 0.3394 \times \xi_C[\%] - 0.001 \times \xi_O[\%] + 1.033 \times \xi_H[\%]$$

with ξ_i as the mass fraction of carbon (C), oxygen (O) and hydrogen (H) in percent.

For diesel fuel, the equation for calculating an LHV estimate based on the volumetric bio-diesel content and the density, suggested by Lopes et al. (2013), was used.

$$LHV_{diesel}\left[\frac{MJ}{kg}\right] = 64.17 - (0.0439 \times \Phi_{biodiesel}[\%]) - \left(25 \times \rho_{diesel}\left[\frac{kg}{m^3}\right]\right)$$

with Φ_i as the volumetric bio-diesel content in % and ρ_{diesel} as the density at 15°C.

APPENDIX 3: STATISTICS OF FUEL SAMPLE DATASET

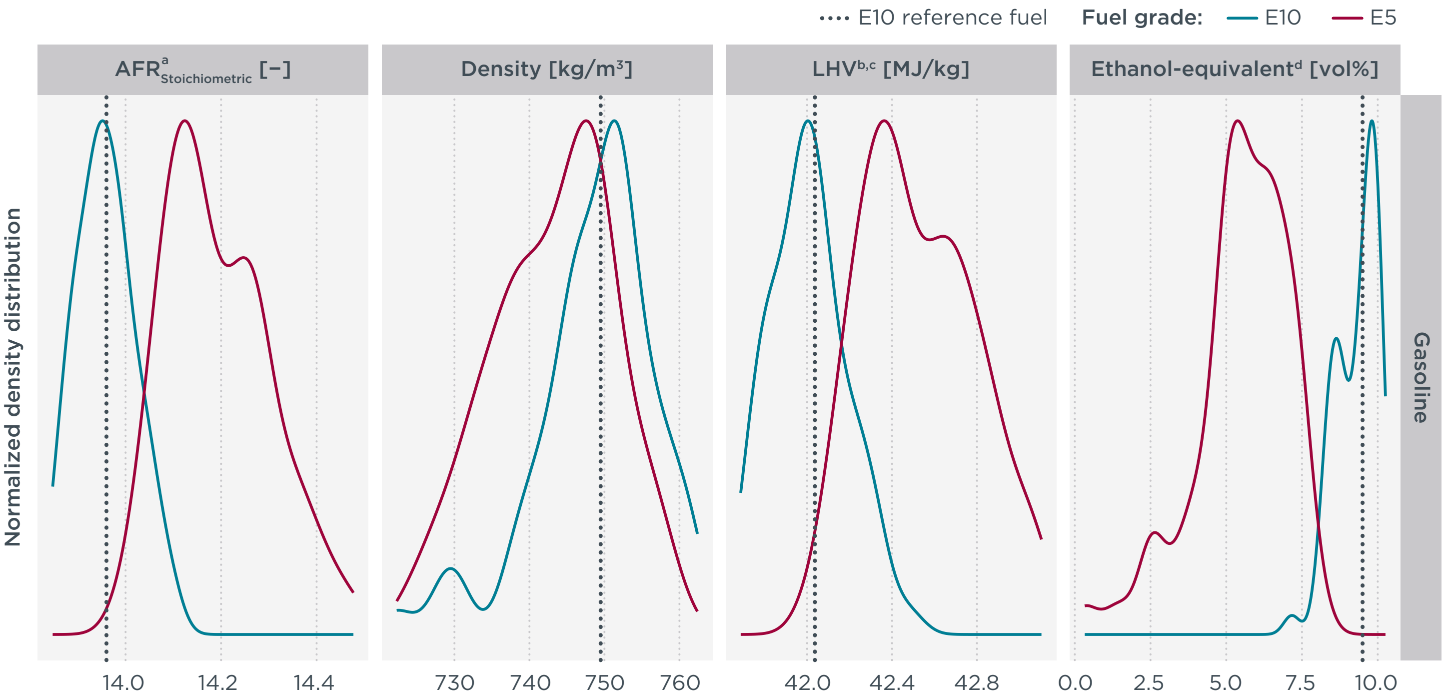

Figure A2. Normalized density distribution of market gasoline E5 and E10 fuel properties, of both summer and winter fuel.

Data source: SGS Germany GmbH.

[a] Stoichiometric air-fuel ratio calculated from fuel composition.

[b] Lower heating value.

[c] For the reference fuel, the lower heating value was also calculated using the formulas provided in Appendix 2.

[d] Considers ethanol, ethyl tertiary-butyl ether (ETBE) and methyl tertiary-butyl ether (MTBE).

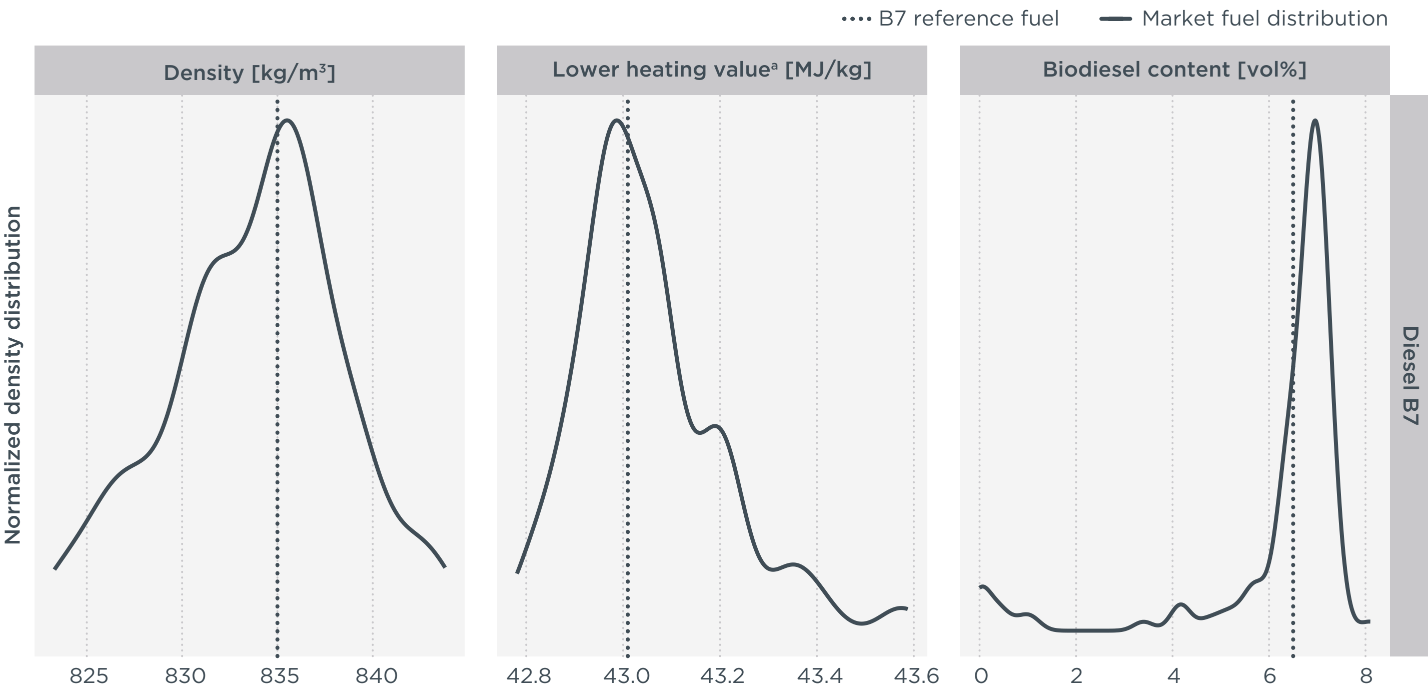

Figure A3. Normalized density distribution of market diesel B7 fuel properties of both summer and winter fuel, excluding artic fuel samples.

Data source: SGS Germany GmbH.

[a] For the reference fuel, the lower heating value was also calculated using the formulas provided in Appendix 2.

APPENDIX 4: CALCULATION OF COMBINED OBFCM UNCERTAINTY

The total OBFCM uncertainty applicable during verification testing was calculated using error propagation rules for multiplicative dependencies as follows.

Total OBFCM fuel consumption real-world error

The theoretical ratio of OBFCM fuel consumption using market fuel, $v_{OBFCM,Market\ fuel}$ and the reference fuel volume, which is the value that would be determined by CVS v_{CVS}, was calculated as follows:

$$rv_{OBFCM,RW} = \frac{v_{OBFCM,Market\ fuel}}{v_{CVS}} = rv_{VM} \times rv_{OBFCM} \times rv_{Fuel\ type}$$

With

» $rv_{VM} = \frac{v_{VM}}{v_{CVS}}$ as the ratio of fuel volume determined by verification method v_{VM} and fuel volume determined by CVS v_{CVS}

» $rv_{OBFCM} = \frac{v_{OBFCM,Reference\ fuel}}{v_{VM}}$ as the ratio of fuel volume determined by OBFCM when using reference fuel $v_{OBFCM,Reference\ fuel}$ and fuel volume determined by verification method rv_{VM}

» $rv_{Fuel\ type} = \frac{v_{OBFCM,Market\ fuel}}{v_{OBFCM,\ Reference\ fuel}}$ as the ratio of fuel volume determined by OBFCM when using market fuel $v_{OBFCM,Market\ fuel}$ and fuel volume determined by OBFCM when using reference fuel $v_{OBFCM,Reference\ fuel}$

Considering the absolute error margin Δrv_i of each ratio rv_i the equation above expands as follows, with Δrv_{OBFCM} as the combined absolute OBFCM uncertainty.

$$(rv + \Delta rv)_{OBFCM} = (rv + \Delta rv)_{VM} \times (rv + \Delta rv)_{OBFCM} \times (rv + \Delta rv)_{Fuel\ type}$$

Applying the error propagation rule for multiplicative dependencies and assuming that the fuel volumes v_{VM}, v_{CVS}, $v_{OBFCM,Maraket\ fuel}$ and $v_{OBFCM,Reference\ fuel}$ are identical except for the random error, meaning that without random errors, the ratios rv_i equal one, the total relative OBFCM fuel consumption error εv_{OBFCM} can be estimated using the following equation.

$$\varepsilon v_{OBFCM} = \frac{\Delta rv_{OBFCM}}{rv_{OBFCM}} = \sqrt{(\Delta rv_{VM}^2 + \Delta rv_{OBFCM}^2 + \Delta rv_{Fuel\ type}^2)} = \Delta rv_{OBFCM}$$

Total OBFCM distance real-world error

Similar to the method described in the previous section, the relative OBFCM distance error εd_{OBFCM} can be estimated.

The calculation takes into account the random errors of verification method and OBFCM device and the effect of tire pressure, dimensions, and tread wear.

$$\varepsilon d_{OBFCM} = \frac{\Delta rd_{OBFCM}}{rd_{OBFCM}} = \sqrt{(\Delta rd_{VM}^2 + \Delta rd_{OBFCM}^2 + \Delta rd_{tire}^2)} = \Delta rd_{OBFCM}$$

With:

» $rd_{VM} = \frac{d_{reference}}{d_{Map}}$ as the ratio of reference distance $d_{reference}$ and distance from electronic map d_{Map}. Applies only for tests performed on public roads where the GPS based distance is used as reference.

» $rd_{OBFCM} = \frac{d_{OBFCM,reference\ tire}}{d_{reference}}$ as the ratio of distance determined by OBFCM using a reference tire at defined pressure $d_{OBFCM,refernece\ tire}$ and the reference distance $d_{reference}$

» $rd_{tire} = \frac{d_{OBFCM}}{d_{OBFCM,reference\ tire}}$ as the ratio of distance determined by OBFCM d_{OBFCM} and the distance determined by OBFCM when using a reference tire at defined pressure $d_{OBFCM,reference\ tire}$

APPENDIX 5: CHASSIS DYNAMOMETER RESULTS

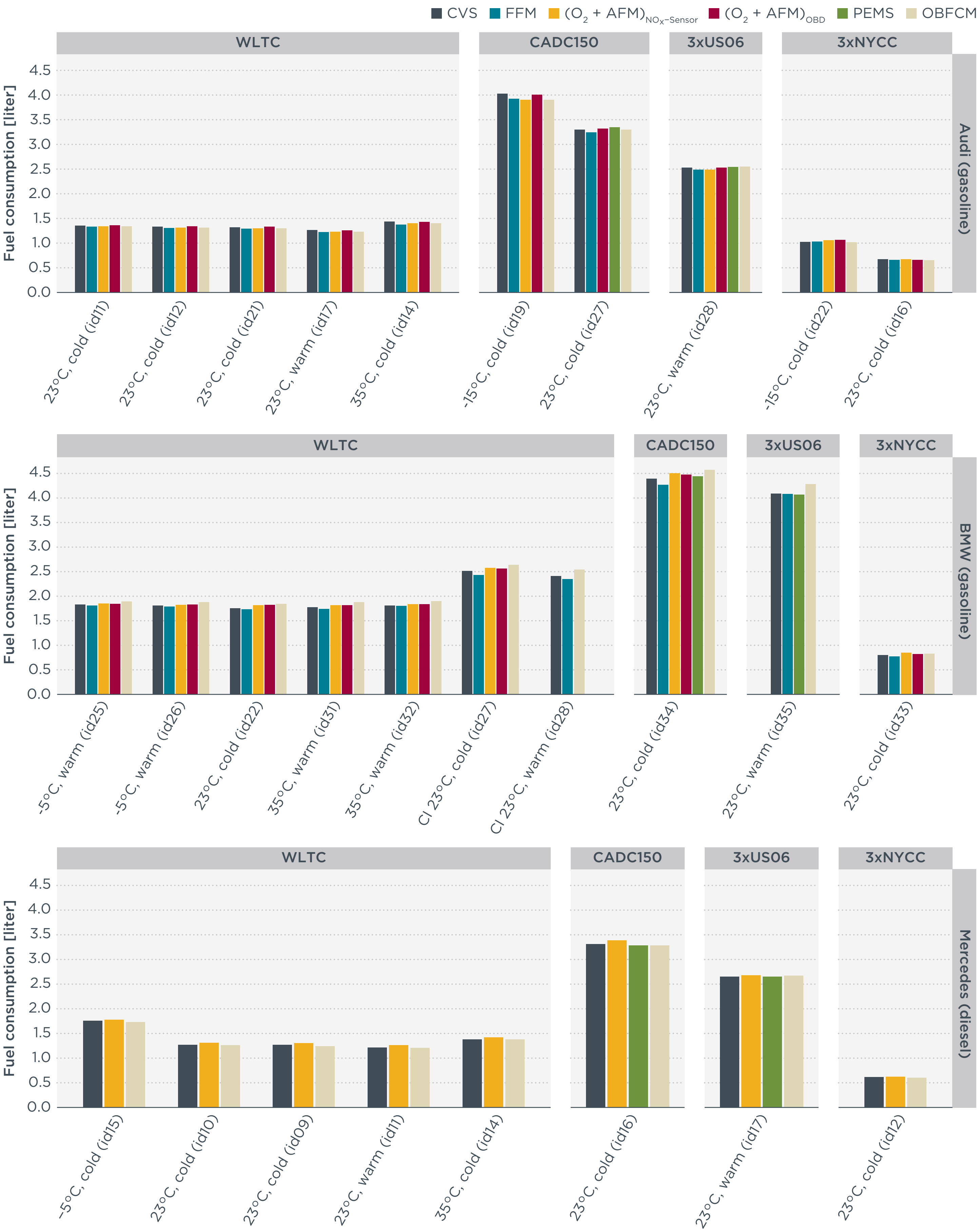

Figure A4. Absolute volumetric fuel consumption of all valid chassis dynamometer tests performed per test vehicle.

APPENDIX 6: CORRECTION OF BMW PEMS EXHAUST MASS FLOW

When processing the BMW RDE test data, we observed a peculiar discrepancy between the fuel volume measured by PEMS and by the other verification methods. It seems to have been caused by an issue with the PEMS exhaust flow meter during the RDE tests. Figure A5 shows the relative error between accumulated PEMS exhaust flow-equivalent air mass flow and the OBD air flow signal for all valid tests performed with PEMS on chassis dyno and on-road. While for the Audi and the Mercedes, the error for tests performed on chassis dyno was similar to the one for on-road tests, a large difference was observed in the BMW test data.

Since the error seemed to be systematic, we adjusted the PEMS exhaust mass flow measured during the RDE tests by the following equation:

$$\dot{m}_{Exh,PEMS,corrected} = \dot{m}_{Exh,PEMS,measured} \times \frac{mean\left(\frac{m_{Air,PEMS}}{m_{Air,OBD}}\right)_{chassis\ dyno\ tests}}{mean\left(\frac{m_{Air,PEMS}}{m_{Air,OBD}}\right)_{on\text{-}road\ tests}}$$

With $\dot{m}_{Exh,PEMS,measured}$ as the exhaust mass flow rate measured during RDE tests, $mean\left(\frac{m_{Air,PEMS}}{m_{Air,OBD}}\right)_i$ being the mean ratio of PEMS equivalent air mass flow and OBD air mass flow during chassis dyno and RDE tests respectively and $\dot{m}_{Exh,PEMS,corrected}$ as the corrected exhaust mass flow.

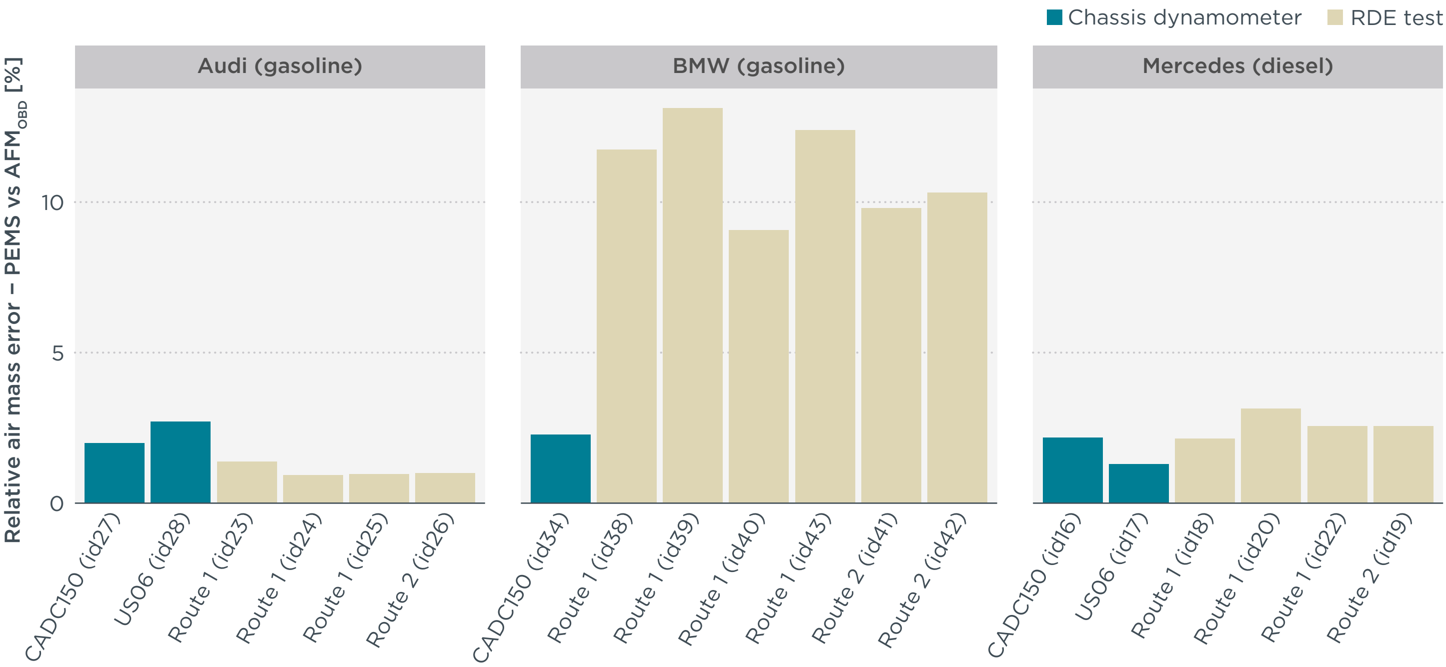

Figure A5. Error between PEMS exhaust flow meter equivalent air mass flow and OBD air mass flow signal measured on chassis dynamometer and during RDE tests. No air mass flow data is available for the BMW 3xUS06 chassis dyno test due to a data acquisition failure.